

## CHAPTER 5

### DESIGN & SIMULATION APPROACH OF PROSTHETIC FOOT

The complete technique for designing and analyzing multiple K-level human foot models is covered in this chapter. For material optimization data, many factors are analyzed on the foot structure model.

#### 5.1 DESIGN APPROACH

Design thinking is a field that combines designer sensibility and approaches with what is technically achievable and what viable commercial tactics may convert into customer value and market potential (Figure 5.1). (Tschimmel, 2012)

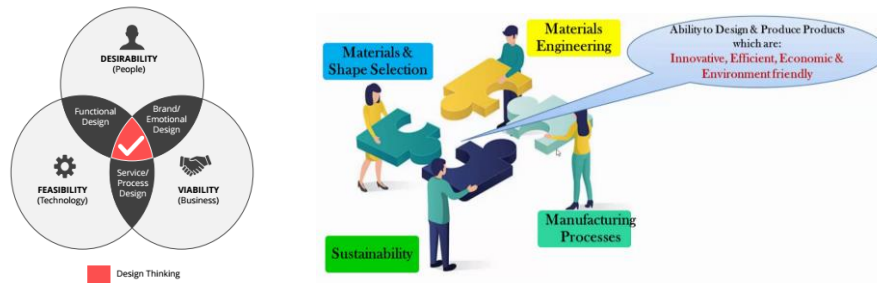


Figure 5.1: Process of design thinking (Meinel & Leifer, 2012)

There is no singular approach to initiating or conceptualizing a design. However, one can seek in a certain direction to find it. Problem identification, user and product research, current brand research, needs and replies and design briefs are a few examples (Figure 5.2).

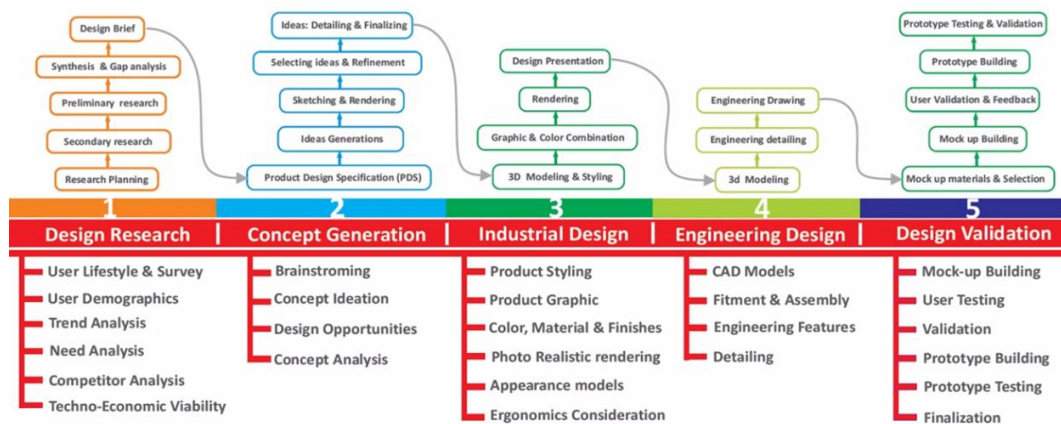


Figure 5.2: Systematic design flowchart

The detailed design and development process of the prosthetic elements is mentioned below in Figure 5.3. This includes research, analysis, and a complete understanding of the end user. (Razzouk & Shute, 2012)

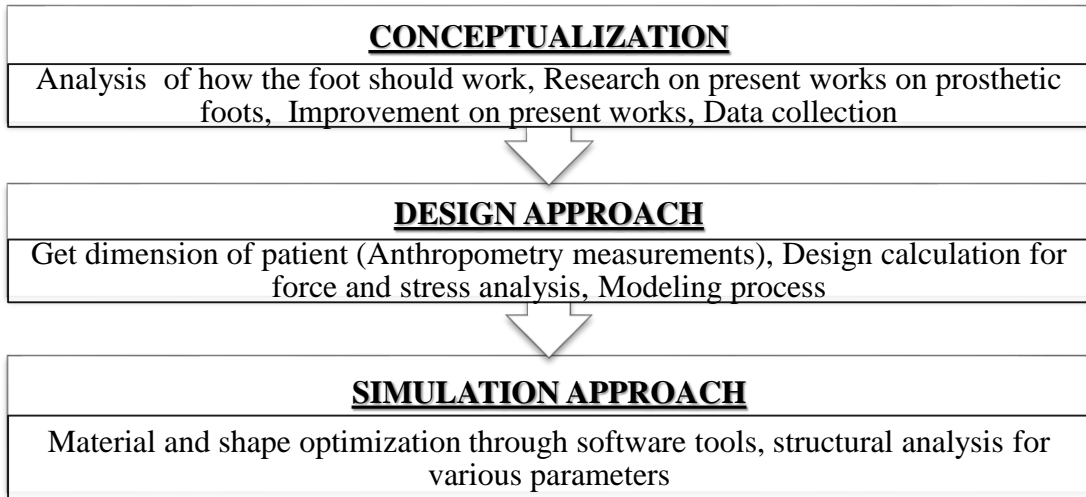


Figure 5.3: Design and simulation flow chart

### 5.2 PARTICIPATORY APPROACH

The purpose of this study is to gather information regarding the present model utilized by patients. Users need access to adaptive hardware that meets specific requirements. Both online surveys and face-to-face interviews were conducted to collect data necessary for the study. A patient survey was conducted as illustrated in Figure 5.4 to Figure 5.7 to obtain background information regarding the use of P&O elements during the visit to the Jaipur foot camp of “bhagwan mahaveer vikalang sahayata samiti” at shree party plot, vashier valley, Valsad on 9<sup>th</sup> January 2020.

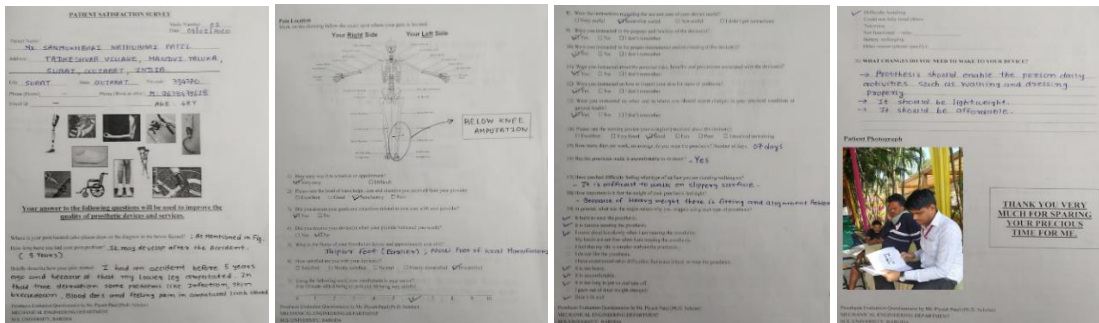


Figure 5.4: Patient feedback form 1

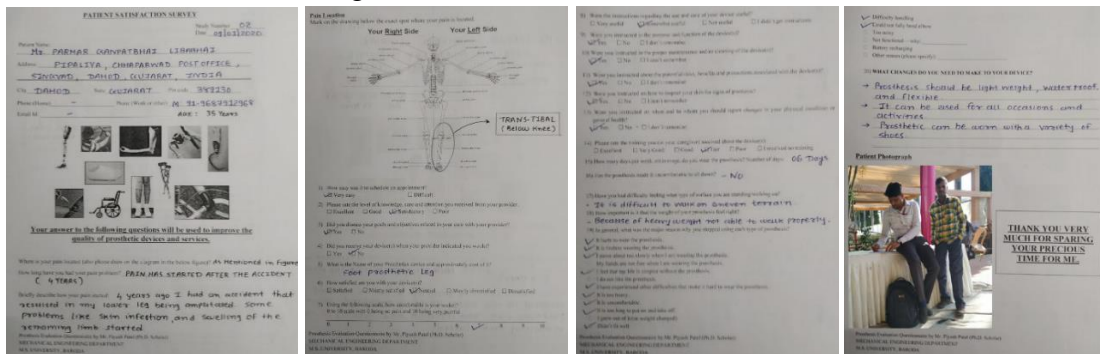


Figure 5.5: Patient feedback form 2

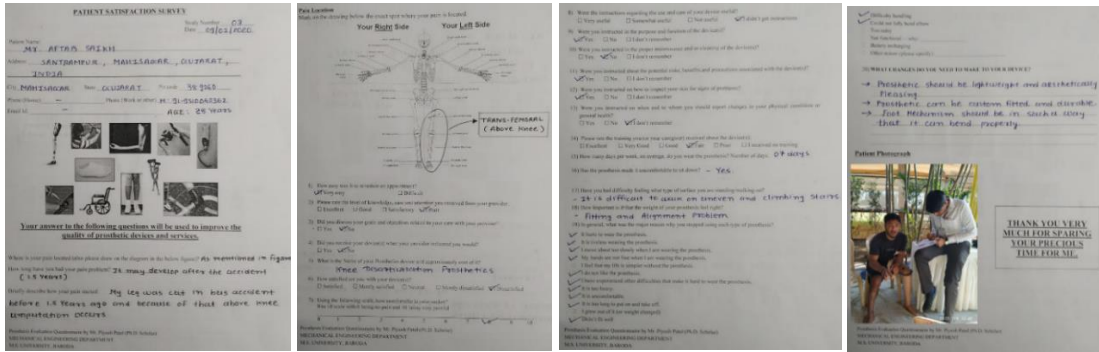


Figure 5.6: Patient feedback form 3

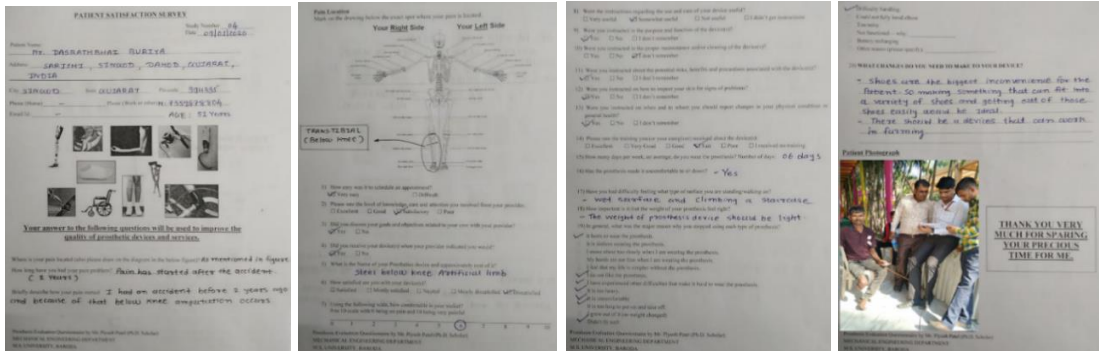


Figure 5.7: Patient feedback form 4

The goal of most new prosthetic designs (Jweeg, Al-Beiruti, & Al-Kinani, 2007) is to replicate natural limb movements as closely as possible, particularly in terms of expected gait patterns (Lenka & Kumar, 2010). In addition, some designs can be made moisture-resistant, making them suitable for shower and beach use, thus enhancing wearer comfort.

However, in many countries components are still imported, especially when it comes to designed and finished prosthetics. Hopefully, this study proposes to fill this gap by showing alternatives for making much cheaper prosthetics. Therefore, affordable prosthetic parts as well as other devices manufactured with economical technology, are certainly in great demand.

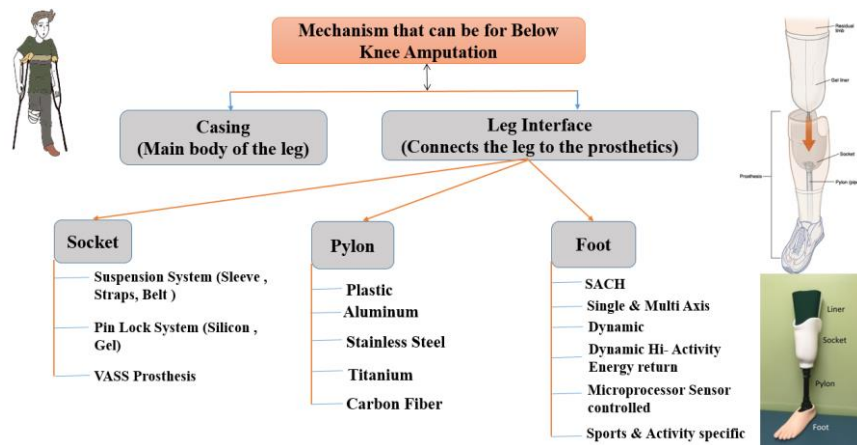


Figure 5.8: Below-knee amputation mechanism

The below-knee prosthetics feature a movable active foot, a solid composite pylon, and a socket connector (Figure 5.8). A pylon is an interior circular tube that attaches to the shaft at the proximal end and holds the amputee's feet at the distal end. The remaining limb socket is a plastic cavity that fits the outer profile of the remaining limb and links the prosthetic to the amputee. (Bartkus, Colvin, & Arbogast, 1994)

Classifying patients based on their normal activities is a requirement before starting the part design. The K-level code method is used to categorize entities (Figure 5.9). The designs of these prosthetics vary according to their different functions.



Figure 5.9: Functional level (K level) of prosthetic users

❖ Project scope

- Create several designs and analyze the optimal design using CAD program/stress analysis
- Developing a prototype
- To design, analyze, and testing of components which is light in weight, low cost, precisely manufactured, and perfectly assembled to perform the intended function
- Create a design that appeals to many people
- Making a design of prosthetic and orthotic devices in such a way that the manufacturing process will be simplified

❖ Realistic constraints

- Every amputation is different and a prosthetic may not be comfortable or suitable for everyone
- 3D printing is possible only on a narrow range of materials

The human factor significantly influences the development of devices intended for use by patients. Human-centered design prioritizes creating solutions that align with users' capabilities, constraints, and requirements. Factors such as environmental conditions and ergonomics exert a substantial influence on the design of human-centric elements.

### 5.3 ALTERNATIVE PROSTHETIC FOOT MODELS DESIGN APPROACHES

To bridge the gap between people's demands (Resan, Ali, Hilli, & Ali, 2011) and what is technologically feasible, along with aligning with a viable commercial strategy that

addresses customer value and market potential, design thinking emerges as a pivotal discipline (Figure 5.10).

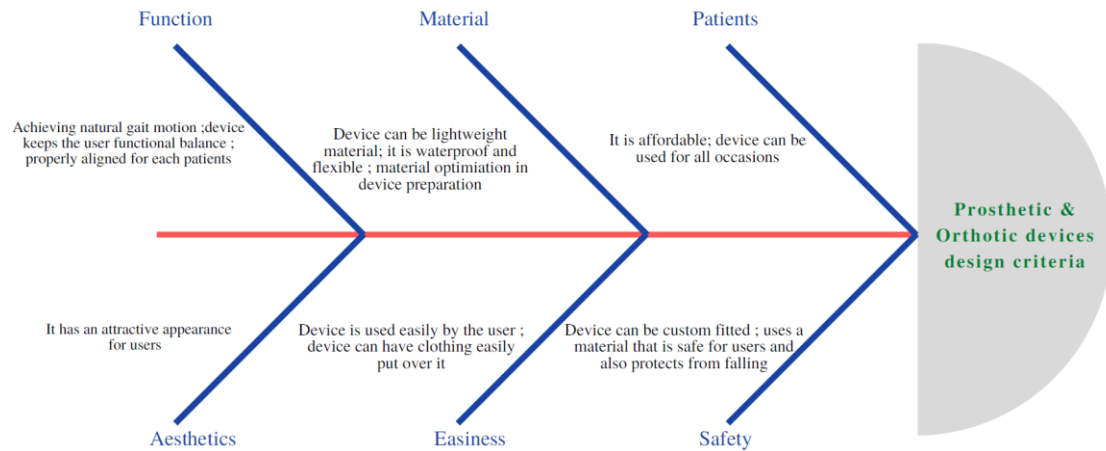


Figure 5.10: Prosthetic and orthotic devices design criteria

Most traditional prosthetics are integral structures, and they cannot be as flexible and convenient as a human foot. The main reason is that human feet are arch-shaped, and their toes can support activities. A bionic mechanical foot is needed to satisfy patients' desire for a highly flexible prosthetic. The design of these prosthetics depends on their functionality. Various configuration models of the prosthetic foot are developed as shown in Figure 5.11 to Figure 5.16.

Differently designed prosthetic feet are well-recognized in the arts (Srikanth & Bharanidaran, 2017). The many conventional designs have attempted to address several prosthetic foot constraints. One limitation associated with prosthetic foot known in the art has to do with manufacturing prosthetic foot having footplates with varying characteristics. Some of the possible variations of a foot plate include width, length, thickness, shape, and stiffness. Incorporating one or more of these variations into the design of a prosthetic can result in a prosthetic with characteristics that are desirable or beneficial for a particular user or particular use. However, incorporating these variations directly into the footplate during the manufacturing process can be expensive, time-consuming, and result in waste of the production materials.

Typically, the prior art multiaxial foot has an axis of rotation via the ankle joint that is transverse to the conventional anterior-posterior alignment of the foot. Such multiaxial prosthetic feet, although often allowing a range of rotation in an anterior-posterior direction, have limited flexibility of movement in a medial-lateral direction. Prior art multiaxial feet often only enable a moderate degree of medial-lateral tilt and do not allow complete rotation in the medial-lateral direction.

As a result, having a prosthetic foot that combines the stability benefits of multi-axial dynamic feet with the energy storage characteristics of a good dynamic foot would be advantageous. Another advantage of employing variable artificial foot is the ability to select a range of medial-lateral rotation and varus-valgus movement for adjusting to uneven terrain, similar to the natural subtalar joint.

The purpose of the first utility model 1 and 2 was to provide a prosthetic foot, based on the existing bionic prosthetic foot, to further improve the cushioning and shock absorption effect of the prosthetic foot on the ground during walking.

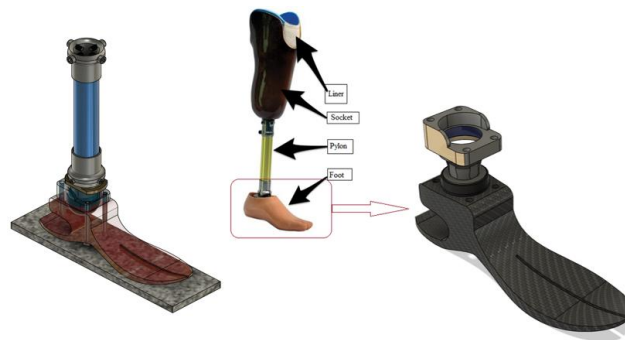


Figure 5.11: Prosthetic foot model 1

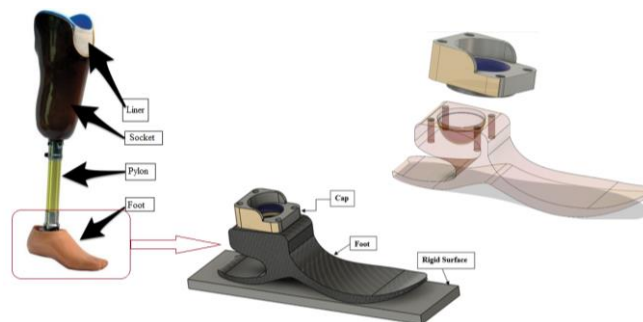


Figure 5.12: Prosthetic foot model 2

The second alternative conceptual design models 3 and 4 were developed to reduce the maximum stress and to increase the strain energy. In the design modification instead of a single unit structure, extra plates were attached to the foot structure mechanism as described in Figure 5.13. A block of rubber imparted some unique properties to the foot piece additionally enabling the amputee to squat.

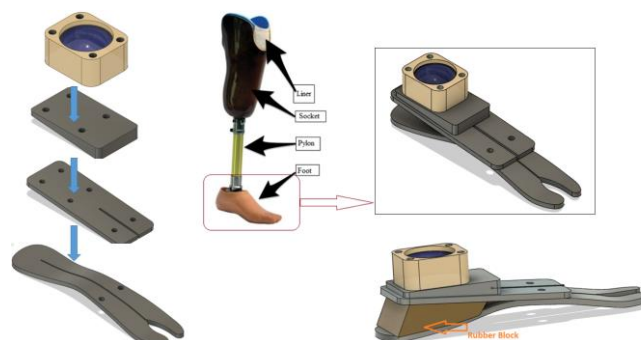


Figure 5.13: Prosthetic foot model 3



Figure 5.14: Prosthetic foot model 4

Due to changes in perspective and much-improved prosthesis technology, many people having physical deficiencies are engaging in a broader range of sports than before.



Figure 5.15: Prosthetic foot model 5



Figure 5.16: Prosthetic foot model 6

Advanced prosthetic devices for running are usually curved blades (Upender, Srikanth, Karthik, & Kumar, 2018) shape as shown in the third alternative conceptual design models 5 and 6 (Figure 5.15 & Figure 5.16). This provides a nice balance of flexibility and strength to withstand high-impact activities like sprinting and jumping.

#### 5.4 SIMULATION APPROACH

Computer simulations were used to assess the performance of prosthetic model 2 during the three primary stages of the gait cycle. These situations included a heel strike (Figure 5.17), a stance phase (Figure 5.18), and a toe-off (Figure 5.19). The most proximal side of the prosthetic was fixed in all three situations, with stresses applied to various sections of the most distal side. (Cahill, 2016)

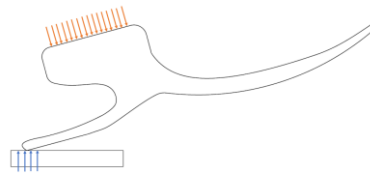
**a) Heel Strike**

Figure 5.17: Prosthetic foot “heel strike” analysis

To imitate the first phase (heel strike) of the three gait phases, ground response forces were given to the most caudal treads. A total floor response force of 1000 N was applied to the prosthetic foot body’s contact zone.

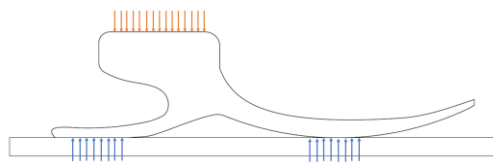
**b) Stance Phase**

Figure 5.18: Prosthetic foot “mid stance” analysis

To simulate the second phase (midstance), a ground force of 1000 N was applied over the entire bottom surface of the prosthetic foot.

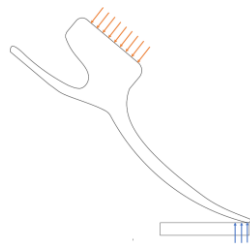
**c) Toe-Off**

Figure 5.19: Prosthetic foot “toe off” analysis

To replicate the last phase (toe-off) of the three gait phases, ground response forces were given to the most caudal treads. A total floor response force of 1000 N was applied to the prosthetic foot body’s contact zone.

The different prosthetic foot analysis (Rochlitz & Pammer, 2017) stages were described to get a basic idea of different load situations. Gait has been separated into parts that allow us to describe, interpret, and assess the events that are taking place. A gait cycle is described as two consecutive occurrences of the same limb, which is frequently the lower extremity’s first contact with the supporting surface.

- a) Prosthetic foot “heel strike” analysis
- b) Prosthetic foot “mid stance” analysis
- c) Prosthetic foot “toe off” analysis

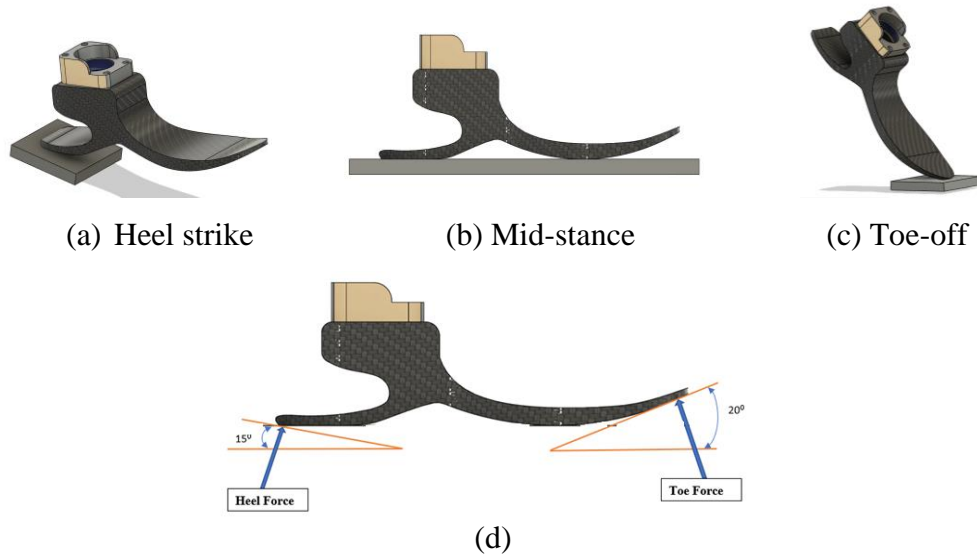


Figure 5.20: Prosthetic foot analysis stages

The platen is inclined at  $-15^\circ$  and  $20^\circ$  angle w.r.to tibia axis to apply loading on the heel and the toe portion respectively as shown in Figure 5.20 (d). Contact settings between the platen and either the heel or toe surface are treated as frictionless without penetration.

Finite Element Analysis (FEA) is then performed discretely, accounting for the three major phases that the human foot goes through during a gait cycle (Figure 5.21). The results for each stage of the methodology have been tabulated and discussed in chronological order below. The first phase (heel strike) simulation data findings for prosthetic foot model 2 were stated first, followed by a detailed explanation. Furthermore, the angle between the platen and the foot was deemed to be  $15^\circ$  during the heel-striking phase.

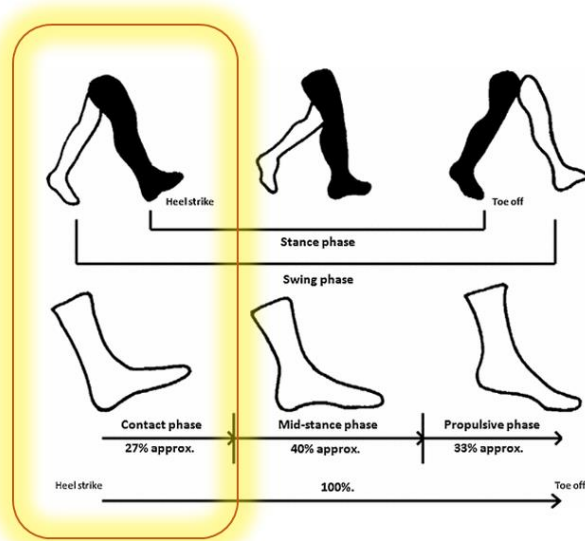


Figure 5.21: Prosthetic foot model 2 in “heel strike” situation

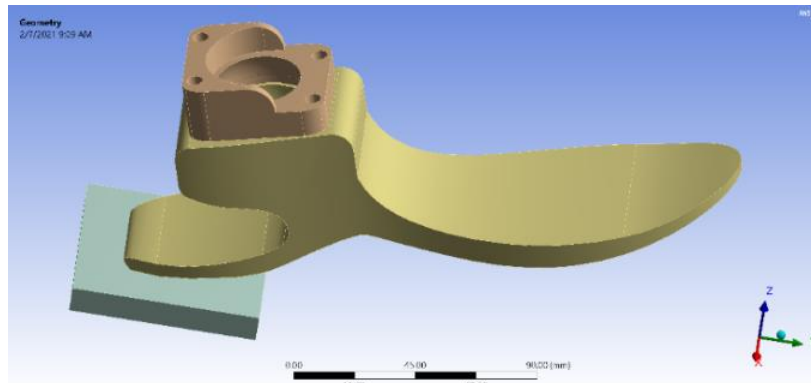


Figure 5.22: Prosthetic foot model 2 geometry during a heel strike situation

An ANSYS Workbench was used to do the FE static structural analysis. ANSYS auto-meshing methods were used to create a FE mesh (Figure 5.23) based on the geometry model (Figure 5.22).

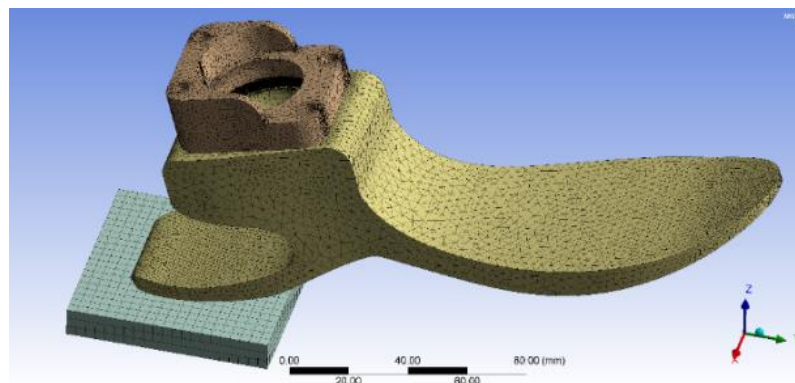


Figure 5.23: Prosthetic foot mesh model 2 during heel strike situation

The main parts of the prosthetic foot model assembly preparation were the mounting bracket and foot structure. The mounting bracket was made from delrin in all configurations of the prosthetic foot models.

The material properties of delrin acetal homopolymer are slightly greater than those of other materials, particularly in large cross-sections. Delrin possesses several properties that make it ideal for mechanical applications and the material of choice for metal part replacement like high strength and stiffness (Kandil, 2016), low friction and wear resistance, high fatigue and creep resistance, chemical resistance, low moisture absorption, temperature toughness, dimensional stability, and overall durability.

Different materials are taken for material analysis of the prosthetic foot model parts preparation like ABS (Acrylonitrile Butadiene Styrene), ABS+PC plastic (Acrylonitrile Butadiene Styrene + Polycarbonate), Acetal homopolymer, CFRC(carbon fiber reinforced composite), nylon 6/6, PEEK (Polyetheretherketone), PET (Polyethylene

terephthalate), PLA (Polylactic acid) and UHMW-PE (Ultra high molecular weight polyethylene).

Frictionless contact between the base plate and the foot cover allowed the prosthetic to flex freely. The reaction forces in the fixed support at the proximal end of the prosthetic pylon are then determined (Figure 5.24).

Due to the low walking pace, only a static transfer without an inertial effect and the influence of gravity was considered; consequently, the fixed support reaction forces and the Ground Reaction Force (GRF) should be equal in size and opposing in orientation. In the case of the most weight-bearing scenario, a vertical force of 1000 N was given to the foot. (Omasta, Paloušek, Návrat, & Rosický, 2012)

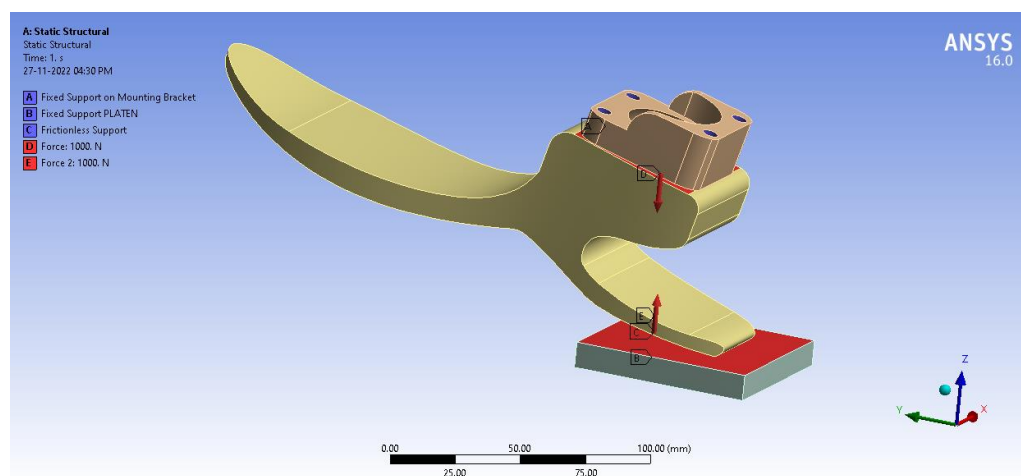


Figure 5.24: Static structural simulation of prosthetic foot model 2 during heel strike situation

Table 5.1: Heel strike analysis on prosthetic foot model 2

Sr no.	Materials	Total deformation (Hz)	Total deformation (mm)	Equivalent stress (MPa)	Strain energy (mJ)
1	ABS	179.65	0.01028	8.0485	0.00098609
2	ABS+PC PLASTIC	178.19	0.009793	8.0528	0.00093959
3	ACETAL RESIN	169.89	0.0085314	8.0697	0.00082101
4	CFRC	213.57	0.002867	14.553	0.00028197
5	NYLON 6/6	135.19	0.016631	7.9983	0.0015791
6	PEEK	203.18	0.006386	8.0444	0.000611
7	PET	174.16	0.0084673	8.09	0.0008177
8	PLA	196.7	0.007118	8.086	0.000687
9	UHMW-PE	595.85	0.002459	50.798	0.0018742

The findings of the mode shape analysis were obtained by modal analysis. The modal analysis results aided us in determining the natural frequency of the foot at various stages of the gait cycle. Total deformation, equivalent von-mises stress, and strain

energy data for each step were detailed in the timeline below from Figure 5.25 to Figure 5.28.

Simulation results data by considering the optimization in the material for the prosthetic foot model 2 was mentioned below. As per the simulated data (Table 5.1), the UHMW-PE material was suitable for the preparation of the prosthetic foot model 2 for the highest natural frequency (595.85 Hz) and strain energy (0.0018742 mJ) as per the applied loading situation in the heel strike simulation.

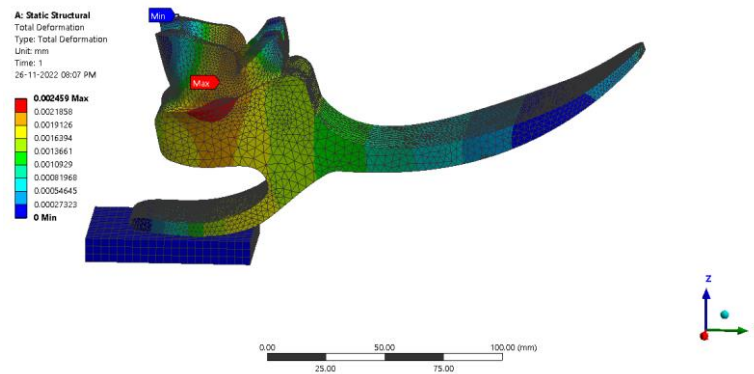


Figure 5.25: Total deformation in mm for prosthetic foot model 2 during heel strike simulation

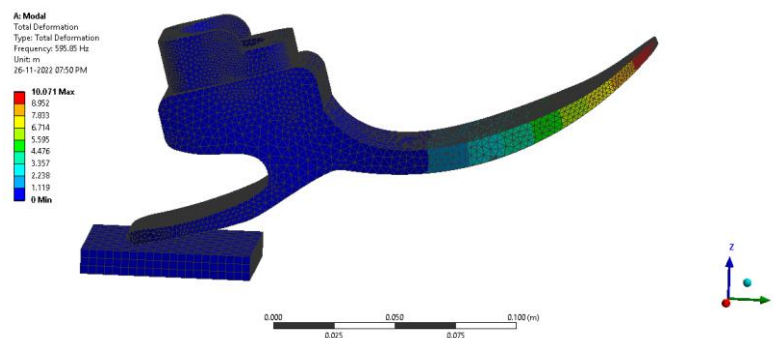


Figure 5.26: Total deformation in Hz for prosthetic foot model 2 during heel strike simulation

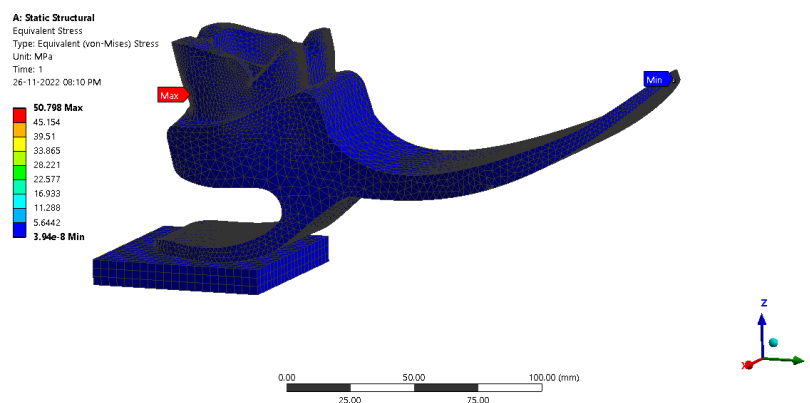


Figure 5.27: Equivalent stress for prosthetic foot model 2 during heel strike simulation

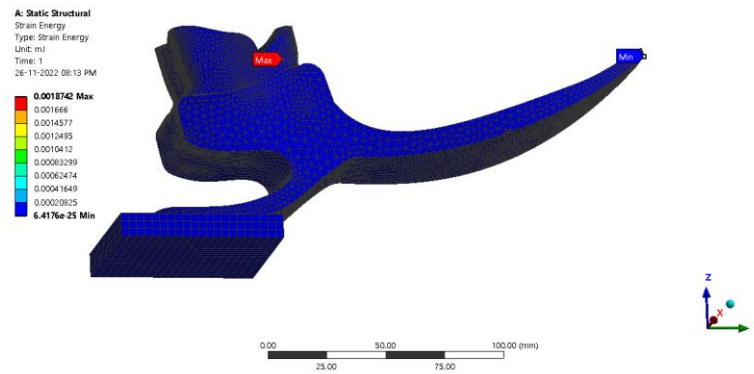


Figure 5.28: Strain energy for prosthetic foot model 2 during heel strike simulation

The midstance phase (Figure 5.29) was reproduced by totally constricting the toe and heel to the platen. A same magnitude vertical load was applied to the foot in a downward motion.

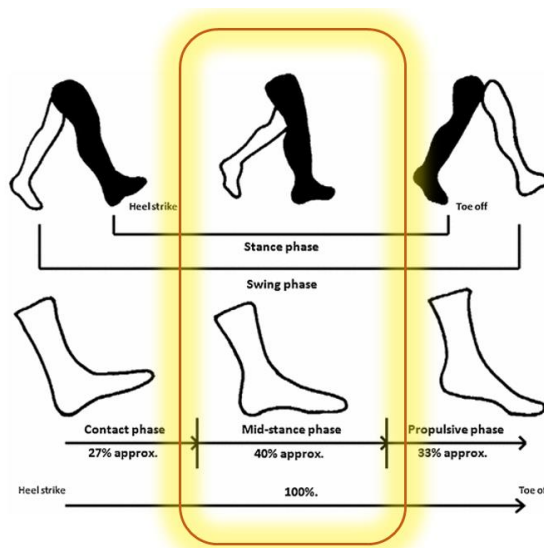


Figure 5.29: Prosthetic foot model 2 in “mid stance” situation

The FE static structural study was performed using an ANSYS Workbench. ANSYS auto-meshing methods were utilized to generate a FE mesh (Figure 5.31) from the geometry model (Figure 5.30).

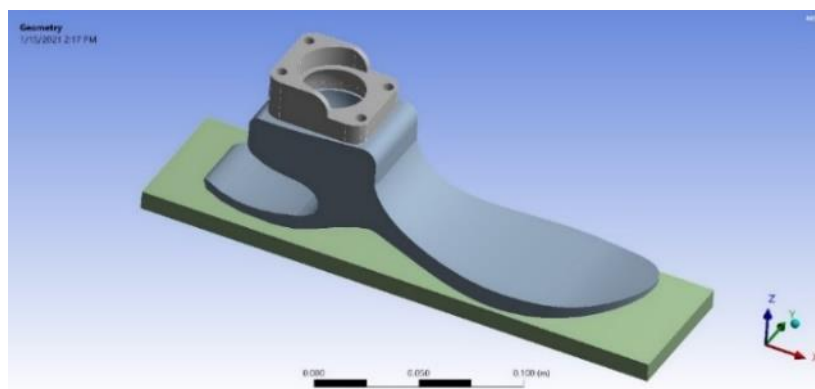


Figure 5.30: Prosthetic foot model 2 geometry during mid stance situation

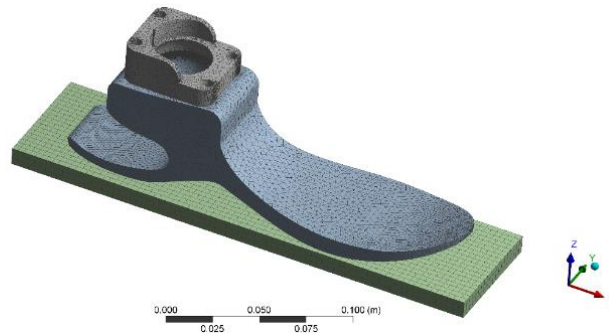


Figure 5.31: Prosthetic foot mesh model 2 during mid stance situation

Figure 5.32 depicts the static structural simulation boundary condition of prosthetic foot model 2 during midstance.

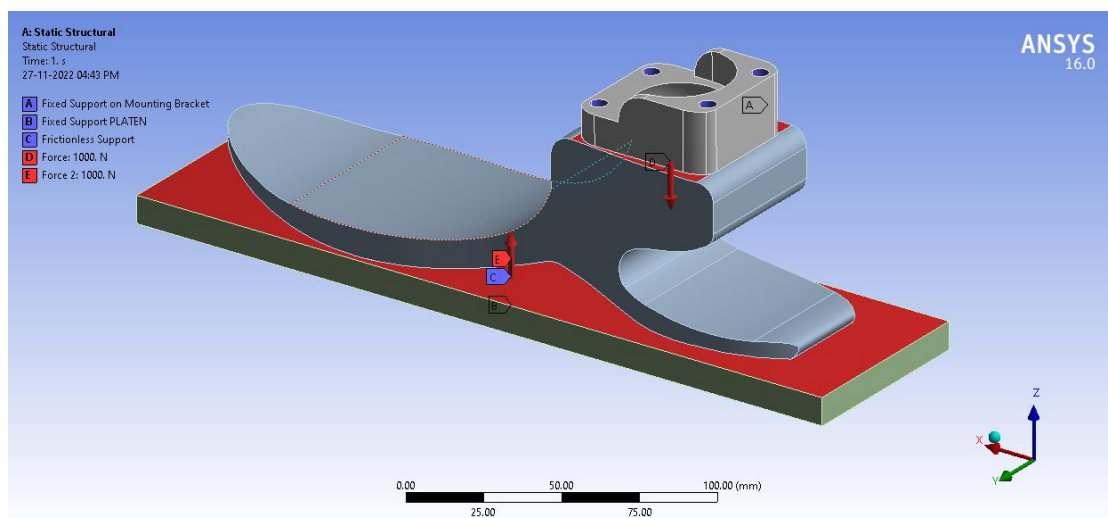


Figure 5.32: Static structural simulation of prosthetic foot model 2 during mid stance situation

Table 5.2: Mid stance analysis on prosthetic foot model 2

Sr. no.	Materials	Total deformation (Hz)	Total deformation (mm)	Equivalent stress (MPa)	Strain energy (mJ)
1	ABS	446.56	0.09735	8.9925	0.002324
2	ABS+PC PLASTIC	443.01	0.09693	8.9863	0.002218
3	ACETAL RESIN	422.71	0.09587	8.9686	0.001946
4	CFRC	1078	0.07392	22.691	0.001593
5	NYLON 6/6	335.28	0.10268	9.0049	0.003685
6	PEEK	504.95	0.09409	8.8455	0.001478
7	PET	433.79	0.0958	8.9871	0.001933
8	PLA	489.83	0.09468	8.9266	0.00164
9	UHMW-PE	1363	0.090459	18.284	0.002472

Simulation results data by considering the optimization in the material for the prosthetic foot model 2 was mentioned in Table 5.2 and static structural analysis data were shown

in Figure 5.33 to Figure 5.36. As per the simulated data, the UHMW-PE material was suitable for the preparation of the prosthetic foot model 2 as per the applied loading situation in the midstance simulation.

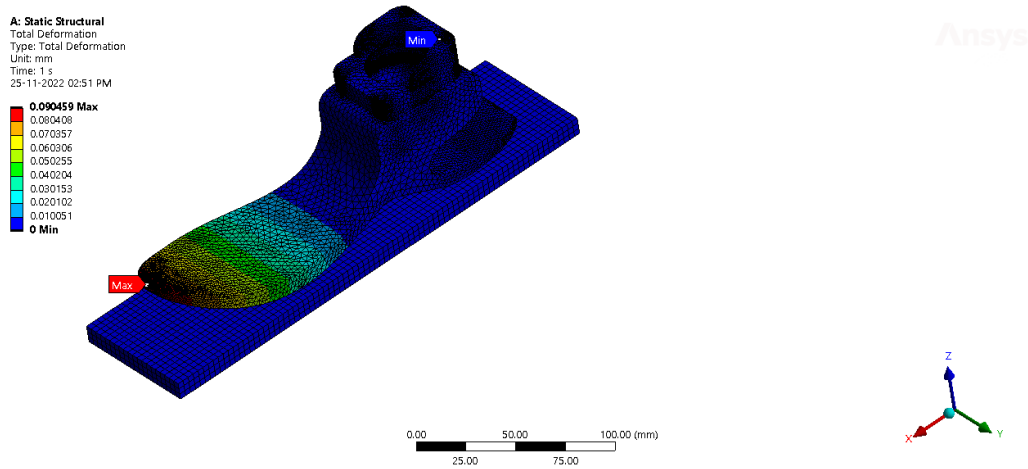


Figure 5.33: Total deformation in mm for prosthetic foot model 2 during mid stance simulation

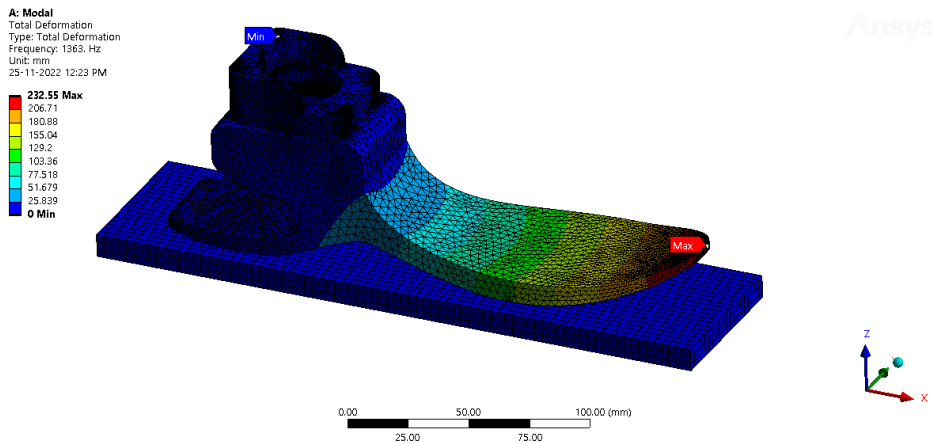


Figure 5.34: Total deformation in Hz for prosthetic foot model 2 during mid stance simulation

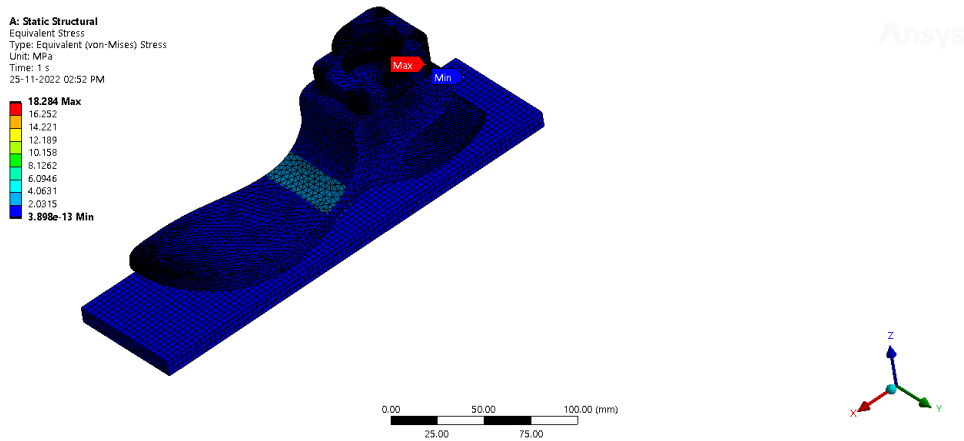


Figure 5.35: Equivalent stress for prosthetic foot model 2 during mid stance simulation

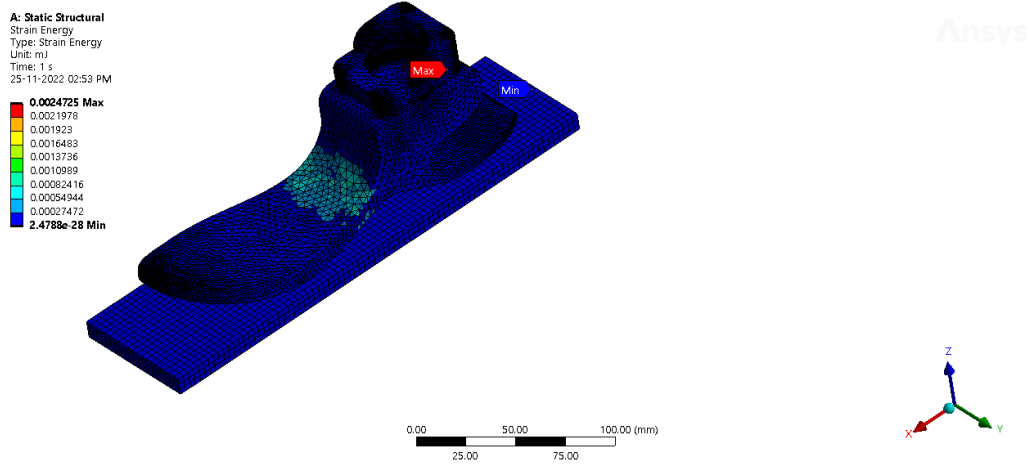


Figure 5.36: Strain energy for prosthetic foot model 2 during mid stance simulation

The toe lift-off phase was reproduced by confining the toe to one of the platens at a 20° angle (Figure 5.37). A comparable vertical force was also applied to the foot as shown in Figure 5.40.

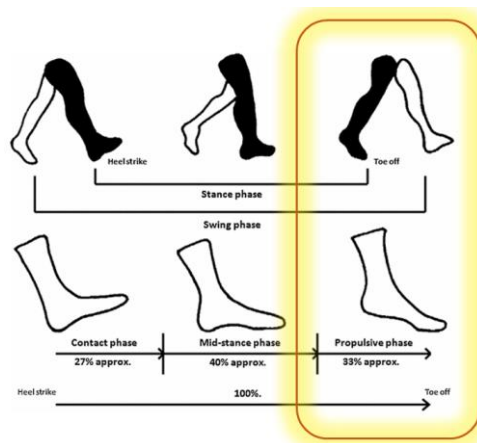


Figure 5.37 Prosthetic foot model 2 in “toe off” situation

An ANSYS Workbench was used to do the FE static structural analysis. ANSYS auto-meshing methods were used to create a FE mesh (Figure 5.39) based on the geometry model (Figure 5.38).



Figure 5.38: Prosthetic foot model 2 geometry during toe off situation

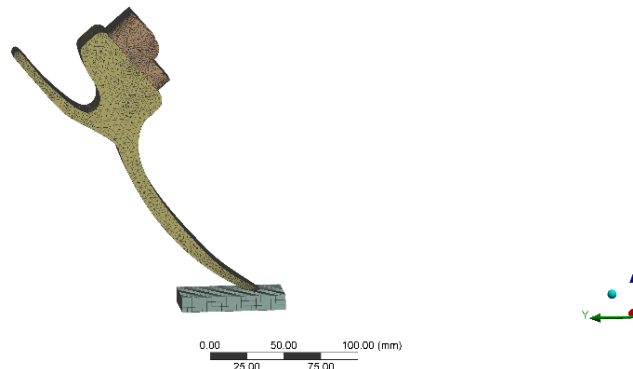


Figure 5.39: Prosthetic foot Mesh model 2 during toe off situation

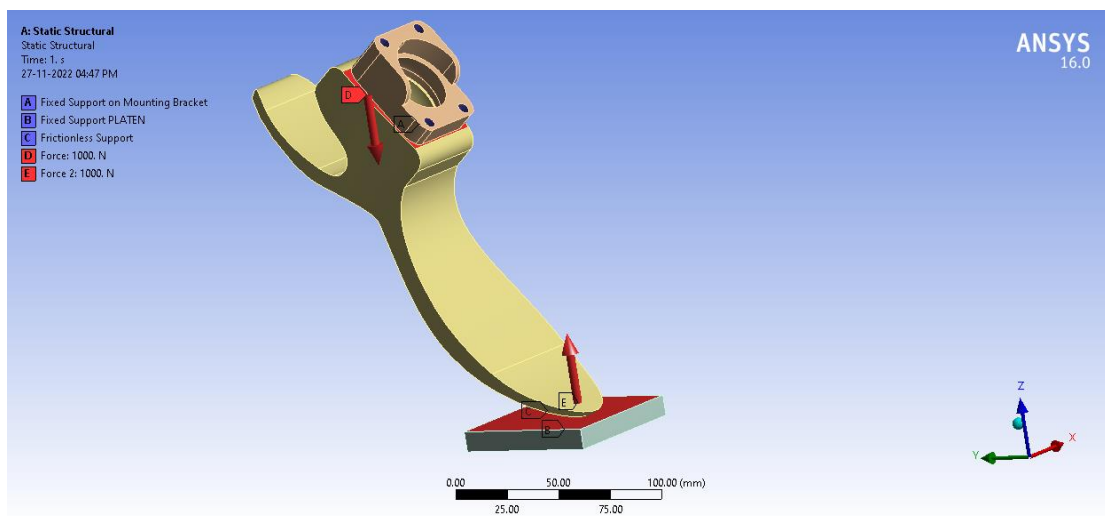


Figure 5.40: Static structural simulation of prosthetic foot model 2 during toe off situation

Table 5.3: Toe off analysis on prosthetic foot model 2

Sr no.	Materials	Total deformation (Hz)	Total deformation (mm)	Equivalent stress (MPa)	Strain energy (mJ)
1	ABS	492.04	0.014	16.079	0.00132
2	ABS+PC PLASTIC	487.99	0.0133	16.079	0.001258
3	ACETAL RESIN	465.08	0.01163	16.08	0.001102
4	CFRC	590.54	0.0032	16.21	0.000444
5	NYLON 6/6	370.64	0.02278	16.074	0.00209
6	PEEK	556.54	0.0087	16.115	0.000818
7	PET	476.57	0.01153	16.069	0.0011
8	PLA	538.29	0.0096	16.085	0.000925
9	UHMW-PE	1613.3	0.003536	54.322	0.00263

Simulation results data by considering the optimization in the material for the prosthetic foot model 2 was mentioned in Table 5.3 and static structural analysis data were shown in Figure 5.41 to Figure 5.44. As per the simulated data, the UHMW-PE material was

suitable for the preparation of the prosthetic foot model 2 as per the applied loading situation in the toe-off simulation.

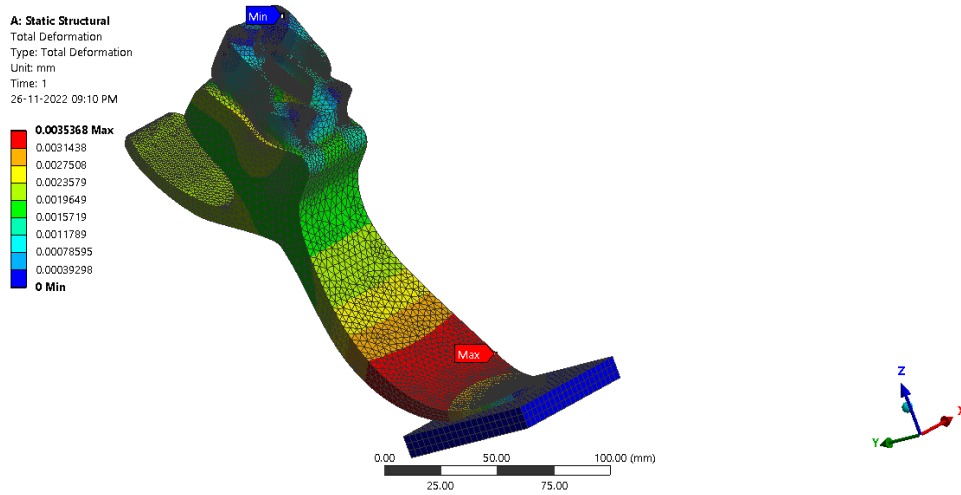


Figure 5.41: Total deformation in mm for prosthetic foot model 2 during toe off simulation

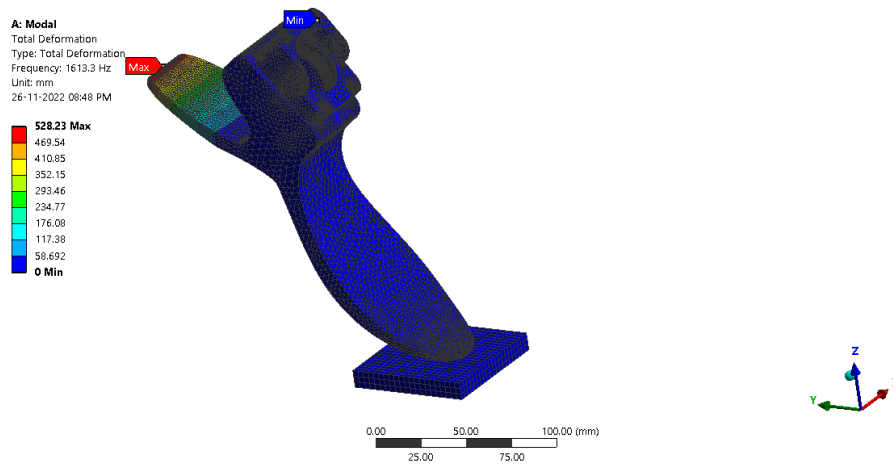


Figure 5.42: Total deformation in Hz for prosthetic foot model 2 during toe off simulation

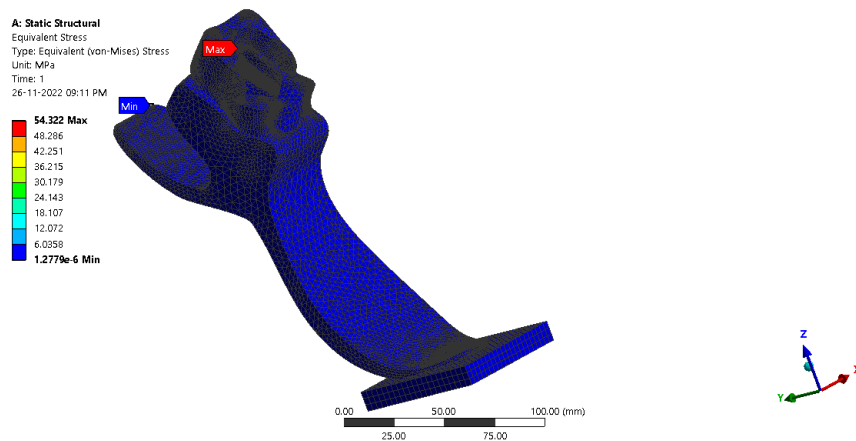


Figure 5.43: Equivalent stress for prosthetic foot model 2 during toe off simulation

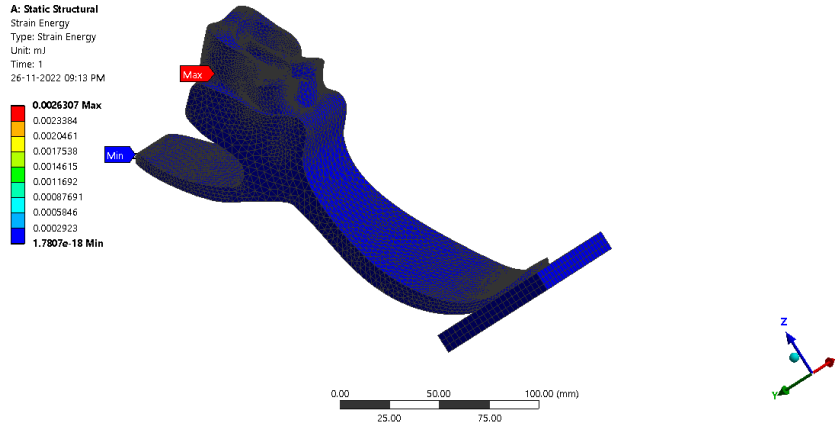


Figure 5.44: Strain energy for prosthetic foot model 2 during toe off simulation

Table 5.4: Frequency analysis of prosthetic foot model 2 for all phases

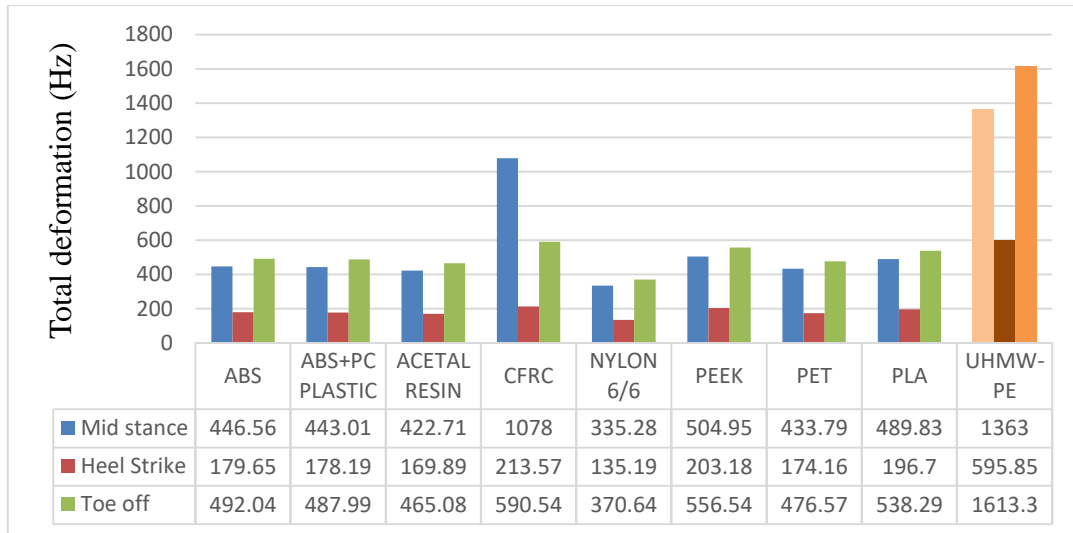


Table 5.5: Deflection analysis of prosthetic foot model 2 for all phases

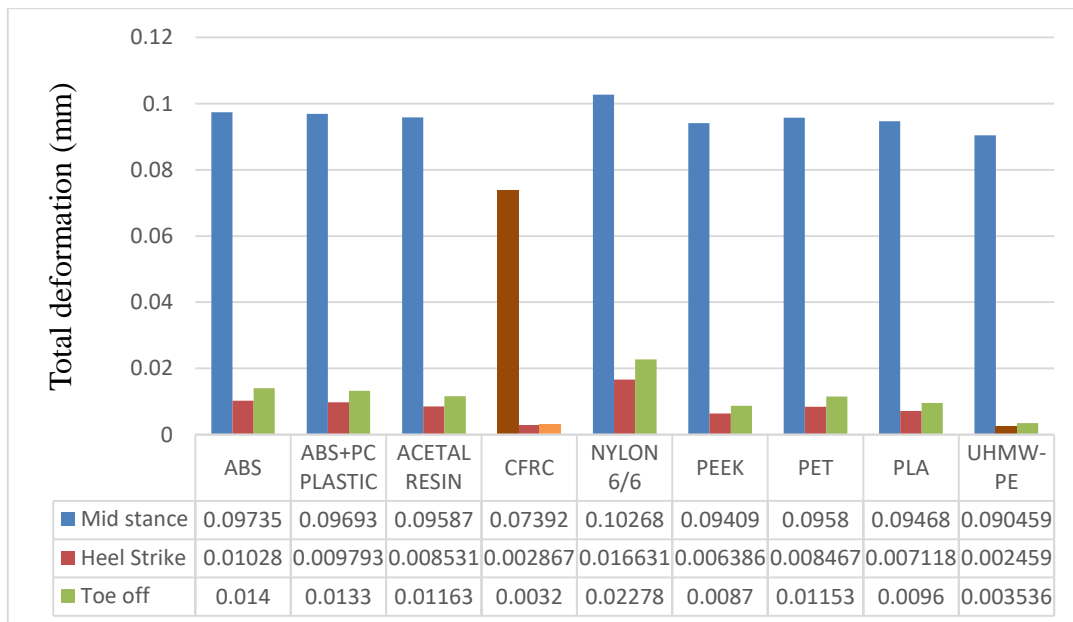


Table 5.6: Stress analysis of prosthetic foot model 2 for all phases

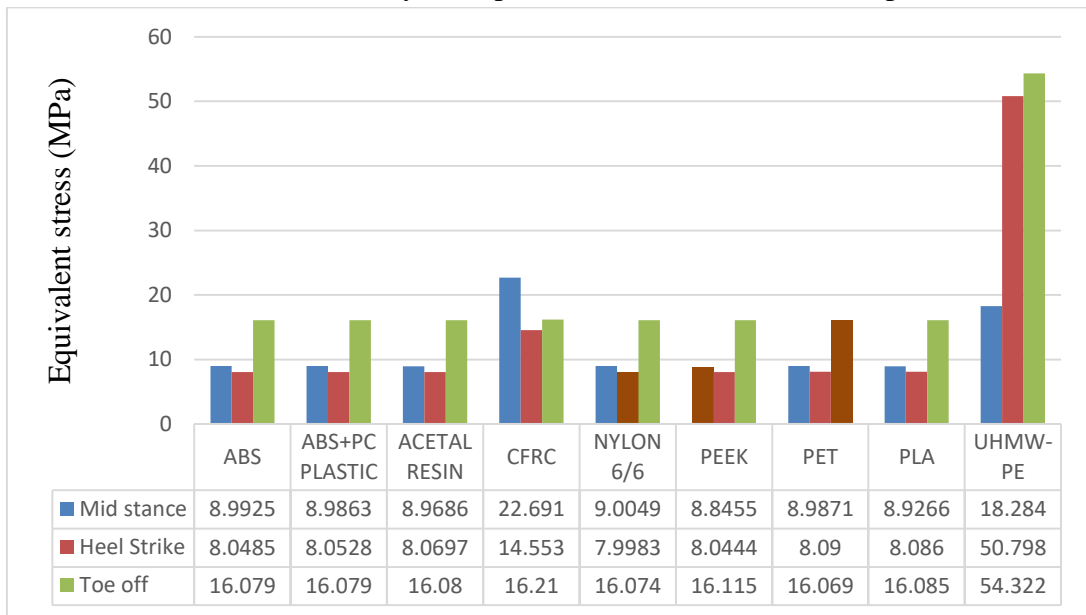
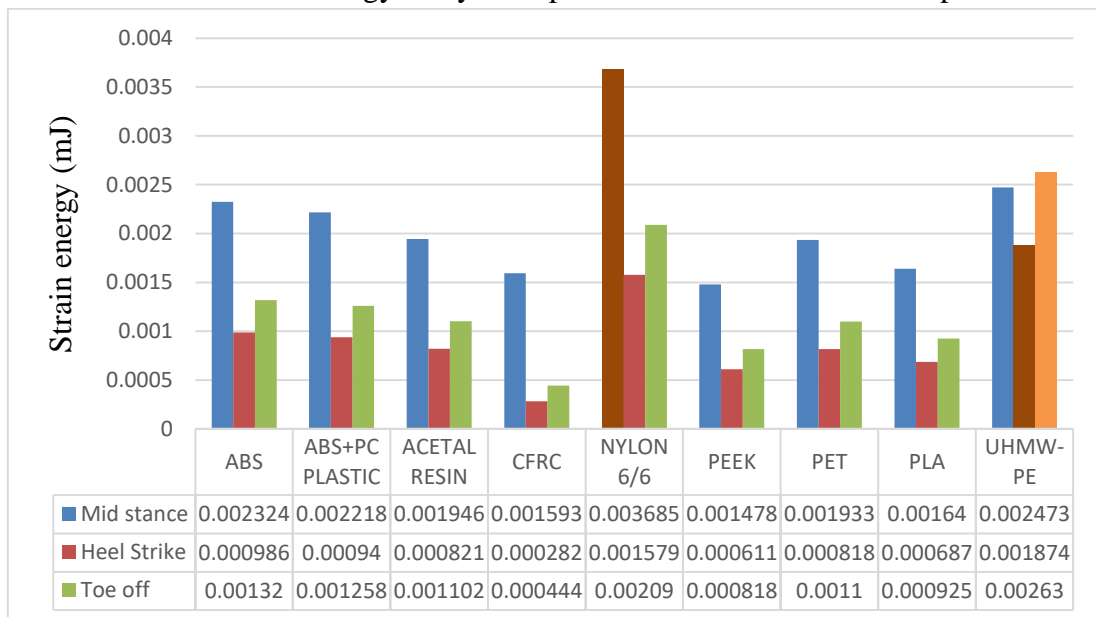


Table 5.7: Strain energy analysis of prosthetic foot model 2 for all phases



According to the static structural and modal analysis of prosthetic foot model 2 for all phases (mid stance/heel strike/toe off), the conclusions are listed as follows;

- 1<sup>st</sup> natural frequency for all phase analyses (midstance /heel strike / toe-off) is very large compared to the average human walking frequency of 2-3 Hz.
- As per different material analysis data;
  - (a) UHMW-PE material has the highest natural frequency for all phase analyses. Natural frequency value for the 1<sup>st</sup> mode in midstance: 1363 Hz; heel strike: 595.85 Hz and toe-off: 1613.3 Hz.

- (b) UHMW-PE material has the highest strain energy in mJ (heel strike: 0.001874; toe-off: 0.00263; mid stance: 0.002472).
- (c) CFRC material has the lowest deformation values compared to other materials in all midstance (0.07392 mm) and toe-off (0.0032 mm) phase analyses and for heel strike (0.002459 mm) UHMW-PE material is suitable.
- (d) PEEK, nylon 6/6, and PET materials are suitable for the lowest average stress value for midstance, heel strike, and toe-off phase analyses.

For prosthetic foot model 1, the midstance phase is replicated by totally restricting the toe and heel to the platen. A same magnitude vertical load is applied to the foot in a downward motion. (Rochlitz, Pammer, & Kiss, Functionality and load-bearing analysis of 3D-printed prosthetic feet, 2018)

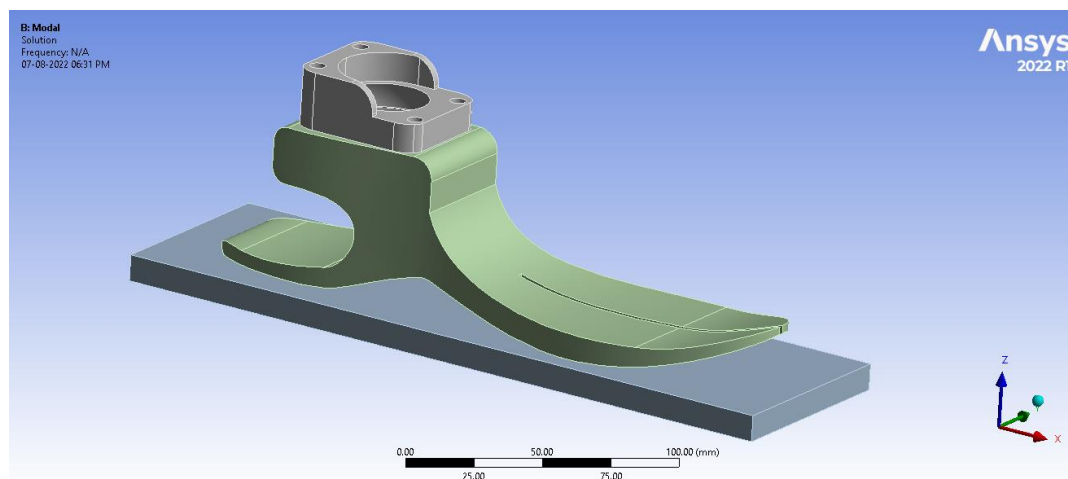


Figure 5.45: Prosthetic foot model 1 geometry during mid stance situation

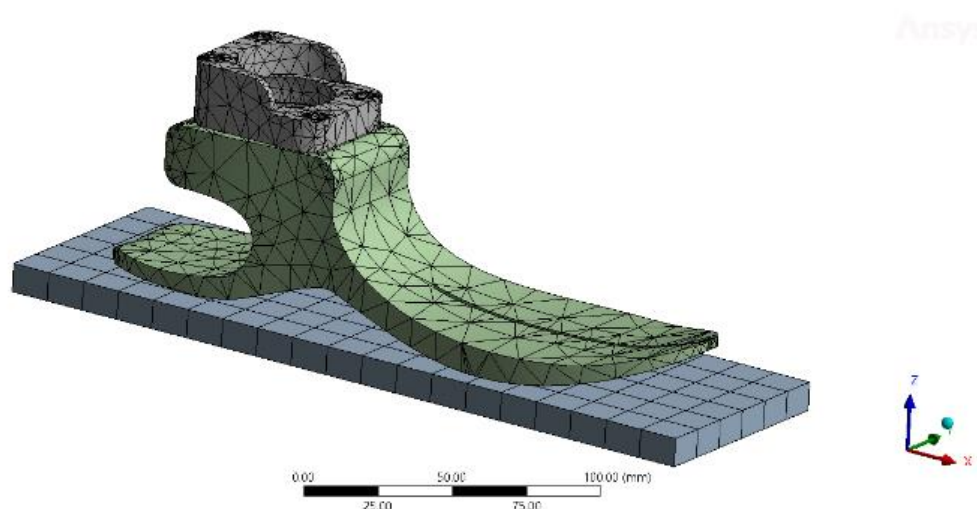


Figure 5.46: Prosthetic foot mesh model 1 during mid stance situation

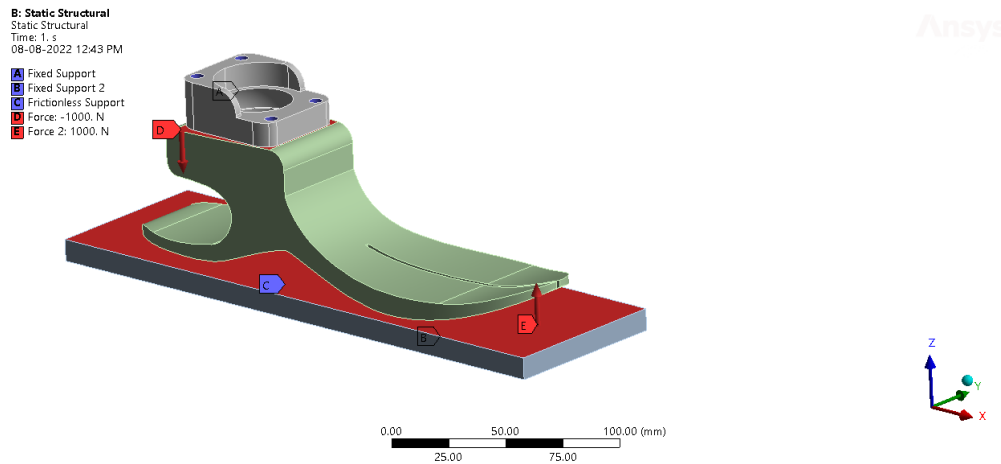


Figure 5.47: Static structural simulation of prosthetic foot model 1 during mid stance situation

Table 5.8: Mid stance analysis on prosthetic foot model 1

Sr no.	Materials	Prosthetic foot model 1			
		Total deformation (Hz)	Total deformation (mm)	Equivalent stress (MPa)	Strain energy (mJ)
1	ABS	1040.5	0.0084	7.5696	0.00694
2	ABS+PC PLASTIC	1031.9	0.00817	7.5486	0.0066
3	ACETAL RESIN	983.41	0.00755	7.4864	0.0059
4	CFRC	4932.2	0.00371	25.289	0.00376
5	NYLON 6/6	783.83	0.01103	7.7744	0.01049
6	PEEK	1176.4	0.0064	9.3241	0.0046
7	PET	1007.8	0.007524	7.4765	0.005896
8	PLA	1138.1	0.006817	8.5308	0.005071
9	UHMW-PE	3429.9	0.0020207	22.761	0.0027462

Simulation results data by considering the optimization in the material for the prosthetic foot model 1 was mentioned in Table 5.8. As per the simulated data, the CFRC material was suitable for the preparation of the prosthetic foot model 1 as per the applied loading situation in the midstance simulation.

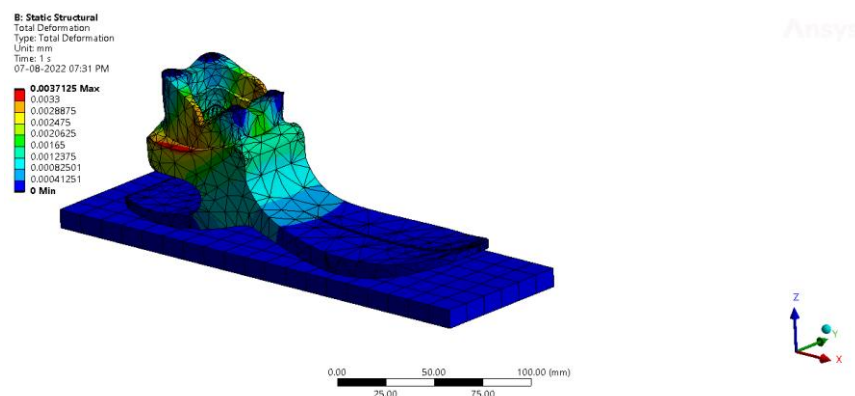


Figure 5.48: Total deformation in mm for prosthetic foot model 1 during mid stance simulation

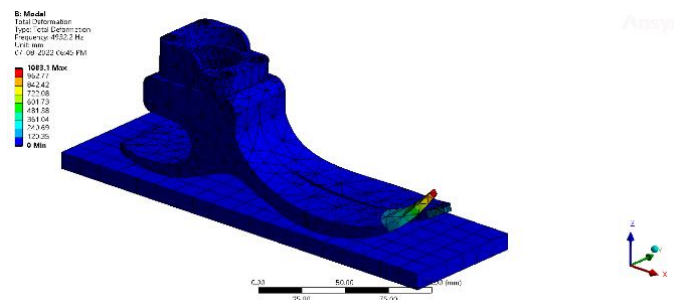


Figure 5.49: Total deformation in Hz for prosthetic foot model 1 during mid stance simulation

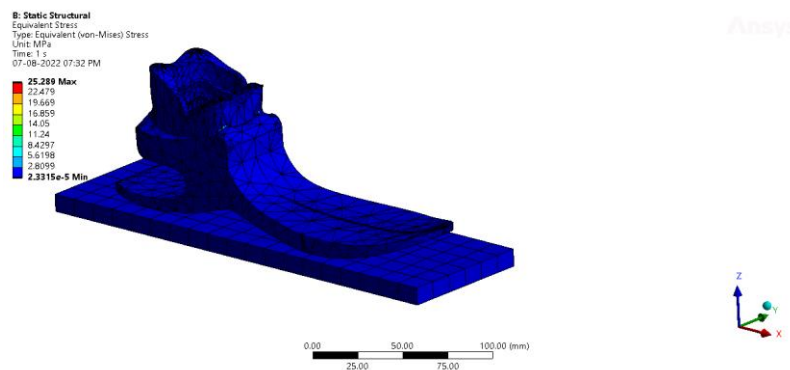


Figure 5.50: Equivalent stress for prosthetic foot model 1 during mid stance simulation

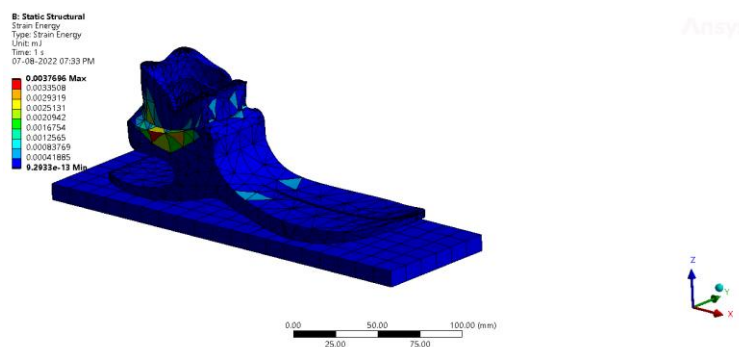


Figure 5.51: Strain energy for prosthetic foot model 1 during mid stance simulation

For prosthetic foot model 3, the mid stance phase was replicated by totally restricting the toe and heel to the platen. A same magnitude vertical load was applied to the foot in a downward motion.

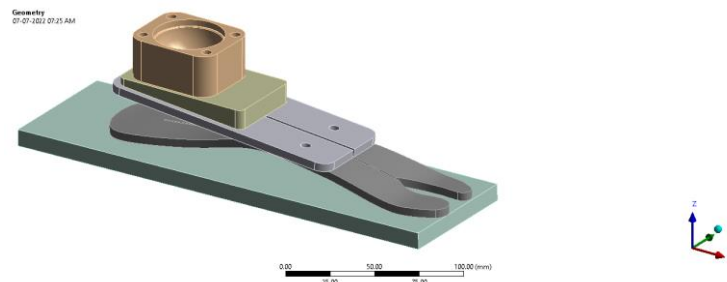


Figure 5.52: Prosthetic foot model 3 geometry during mid stance situation

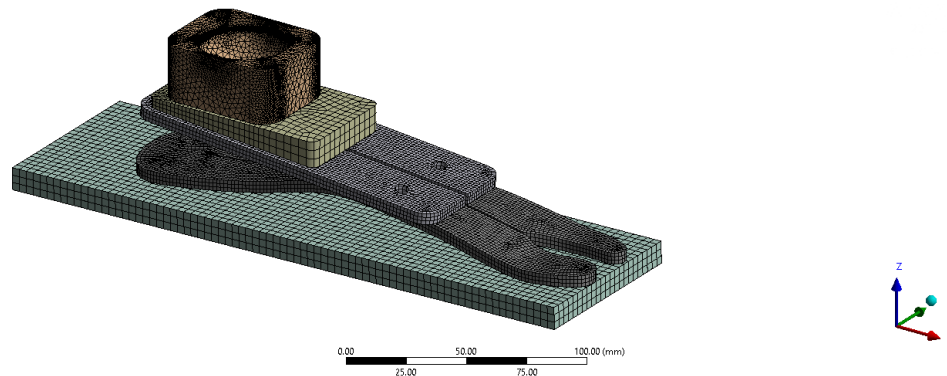


Figure 5.53: Prosthetic foot mesh model 3 during mid stance situation

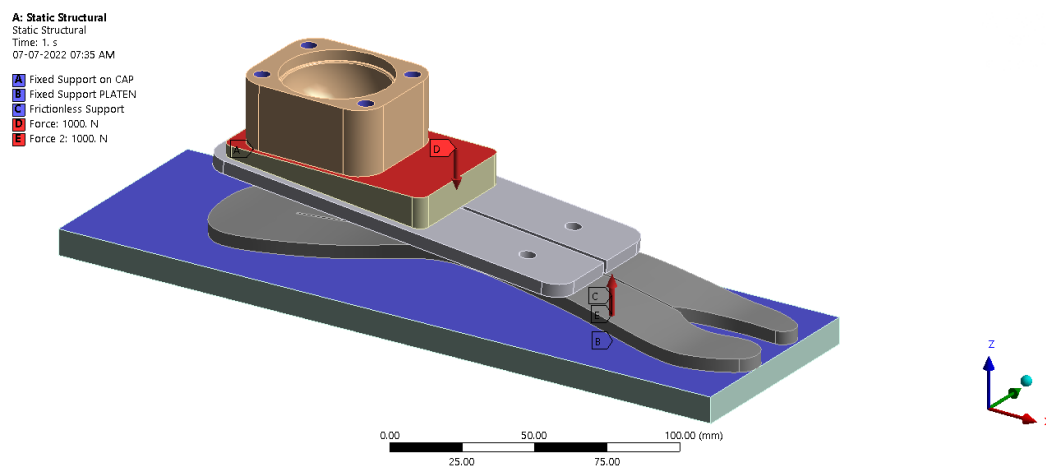


Figure 5.54: Static structural simulation of prosthetic foot model 3 during mid stance situation

Table 5.9: Mid stance analysis on prosthetic foot model 3

Sr no.	Materials	Prosthetic foot model 3			
		Total deformation (Hz)	Total deformation (mm)	Equivalent stress (MPa)	Strain energy (Mj)
1	ABS	663.33	0.0499	6.8566	0.04786
2	ABS+PC PLASTIC	640.42	0.04696	7.375	0.04486
3	ACETAL RESIN	610.35	0.04152	6.8781	0.04001
4	CFRC	3103.1	0.00261	13.566	0.00389
5	NYLON 6/6	486.45	0.07561	9.5337	0.07011
6	PEEK	730.23	0.03191	6.1896	0.03093
7	PET	625.46	0.04131	6.8672	0.04003
8	PLA	706.4	0.035309	6.2459	0.03438
9	UHMW-PE	1913.3	0.0056047	9.428	0.007146

Simulation results data by considering the optimization in the material for the prosthetic foot model 3 was mentioned in Table 5.9. As per the simulated data, the CFRC material was suitable for the preparation of the prosthetic foot model 3 as per the applied loading situation in the midstance simulation.

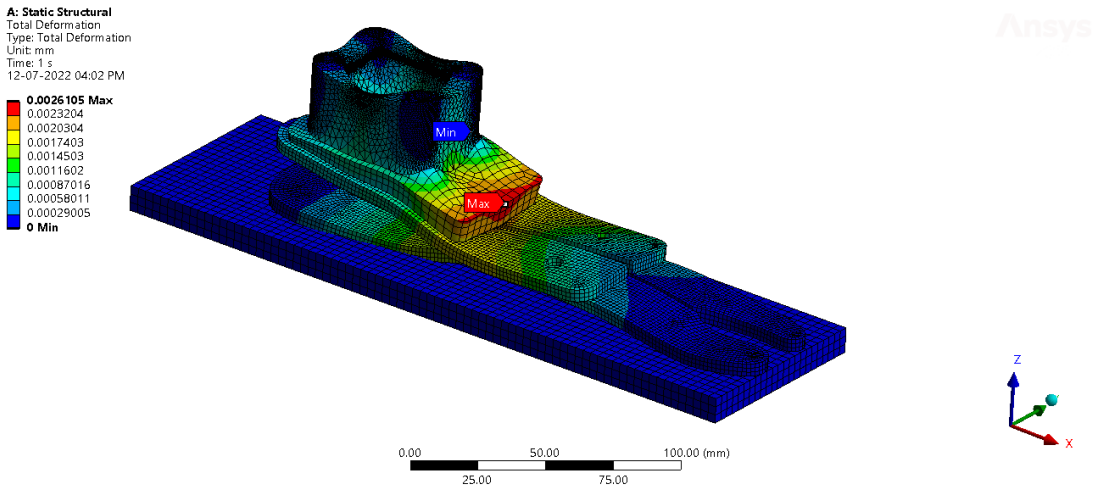


Figure 5.55: Total deformation in mm for prosthetic foot model 3 during mid stance simulation

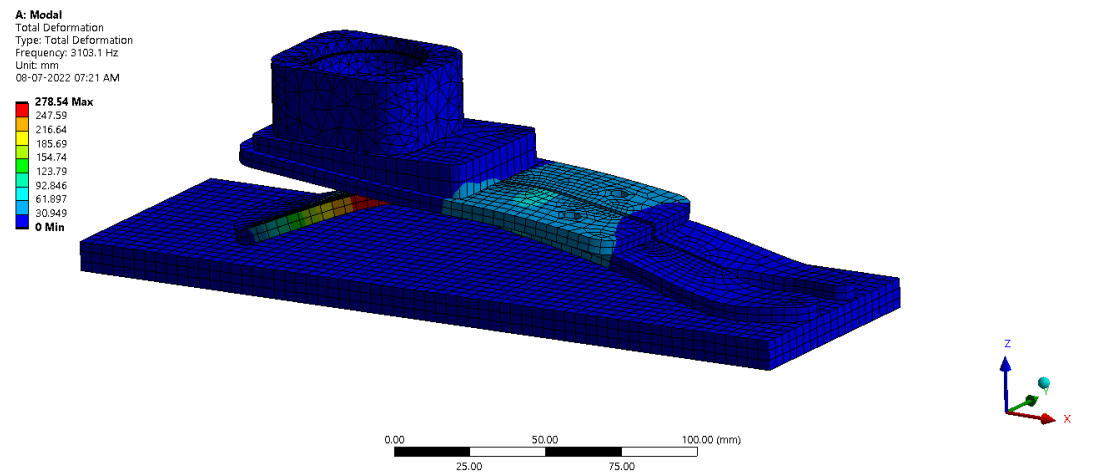


Figure 5.56: Total deformation in Hz for prosthetic foot model 3 during mid stance simulation

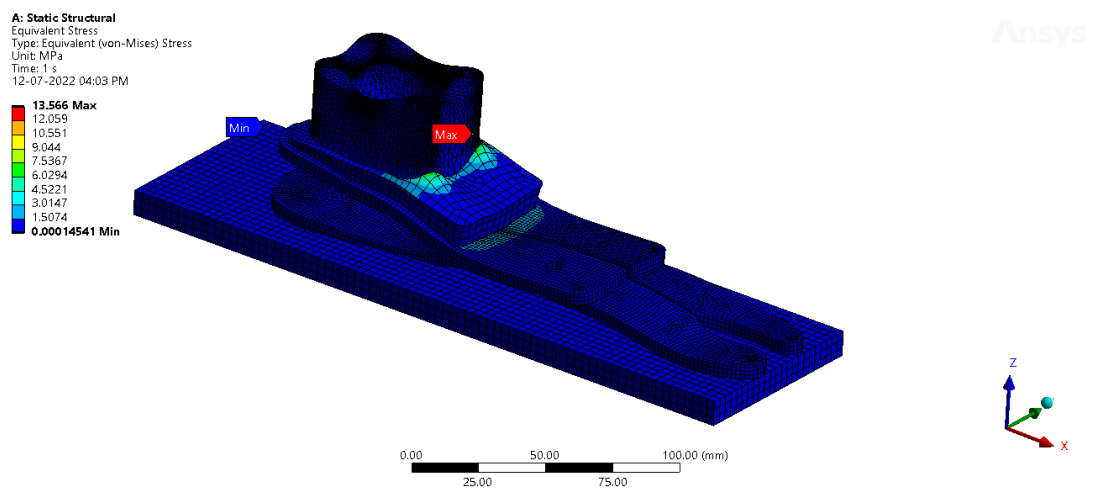


Figure 5.57: Equivalent stress for prosthetic foot model 3 during mid stance simulation

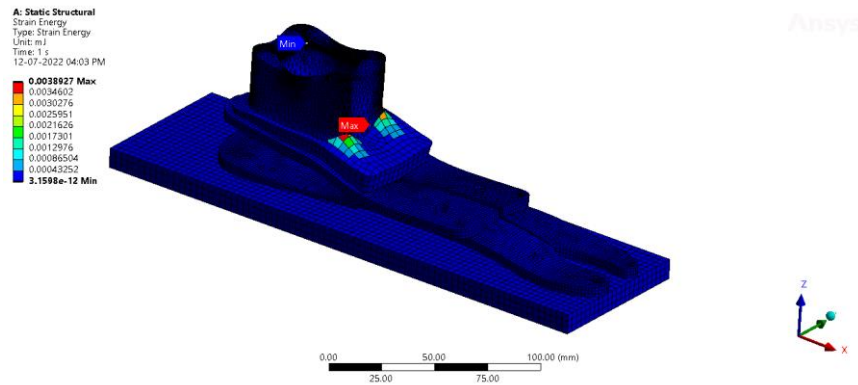


Figure 5.58: Strain energy for prosthetic foot model 3 during mid stance simulation

For prosthetic foot model 4, the mid stance phase was replicated by totally restricting the toe and heel to the platen. A same magnitude vertical load was applied to the foot in a downward motion.

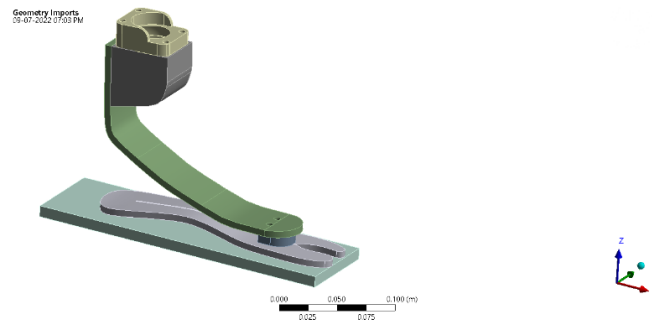


Figure 5.59: Prosthetic foot model 4 geometry during mid stance situation

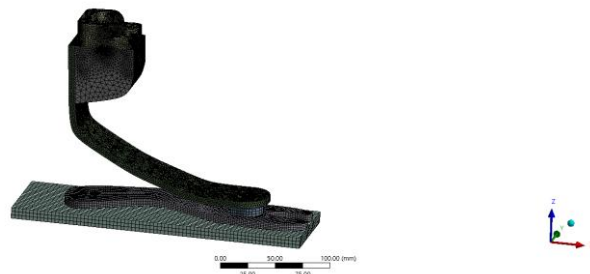


Figure 5.60: Prosthetic foot mesh model 4 during mid stance situation

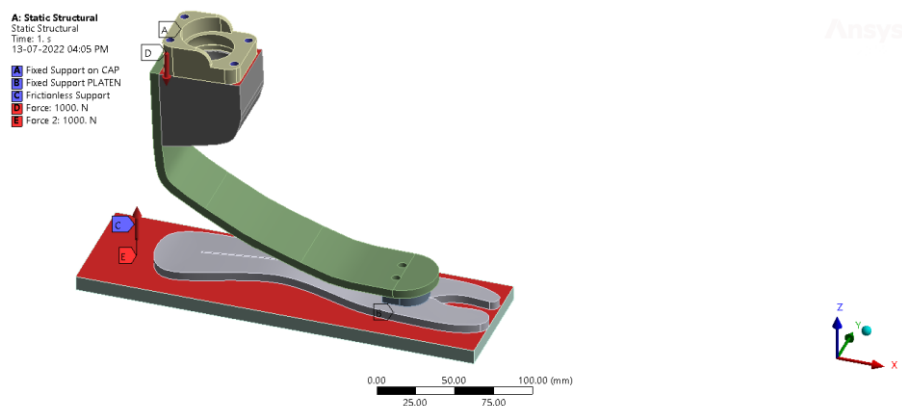


Figure 5.61: Static structural simulation of prosthetic foot model 4 during mid stance situation

Table 5.10: Mid stance analysis on prosthetic foot model 4

Sr no.	Materials	Prosthetic foot model 4			
		Total deformation (Hz)	Total deformation (mm)	Equivalent stress (MPa)	Strain energy (Mj)
1	ABS	471.72	0.00724	7.5111	0.0021
2	ABS+PC PLASTIC	467.82	0.0064	6.9088	0.0016
3	ACETAL RESIN	445.93	0.006	7.535	0.001745
4	CFRC	1119.5	0.00377	22.354	0.003536
5	NYLON 6/6	363.27	0.0087	6.8246	0.0015
6	PEEK	526.14	0.00524	9.4593	0.00204
7	PET	456.88	0.00599	7.5968	0.0017546
8	PLA	511.9	0.00552	8.724	0.001933
9	UHMW-PE	1561.1	0.005997	7.526	0.0017359

Simulation results data by considering the optimization in the material for the prosthetic foot model 4 was mentioned in Table 5.10. As per the simulated data, UHMW-PE material was suitable for the preparation of the prosthetic foot model 4 as per the applied loading situation in the midstance simulation.

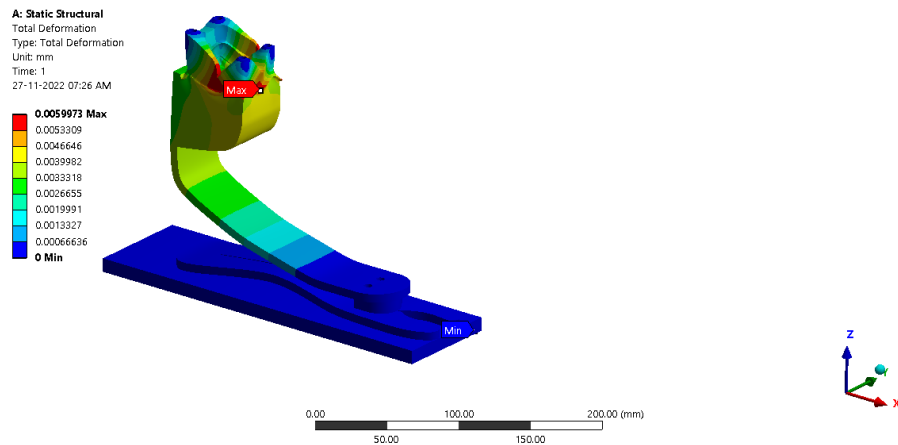


Figure 5.62: Total deformation in mm for prosthetic foot model 4 during mid stance simulation

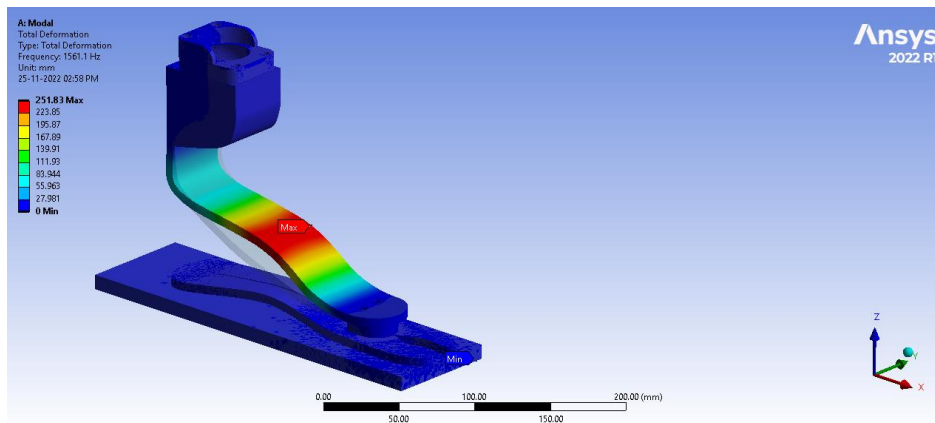


Figure 5.63: Total deformation in Hz for prosthetic foot model 4 during mid stance simulation

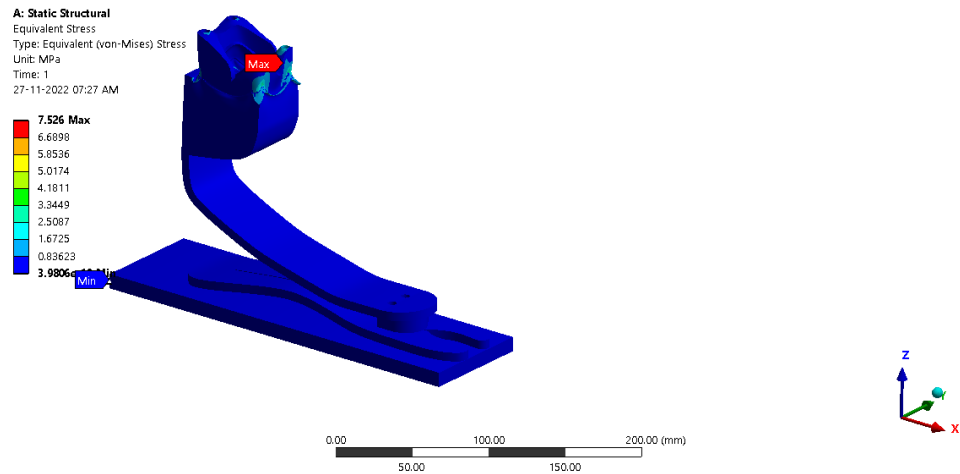


Figure 5.64: Equivalent stress for prosthetic foot model 4 during mid stance simulation

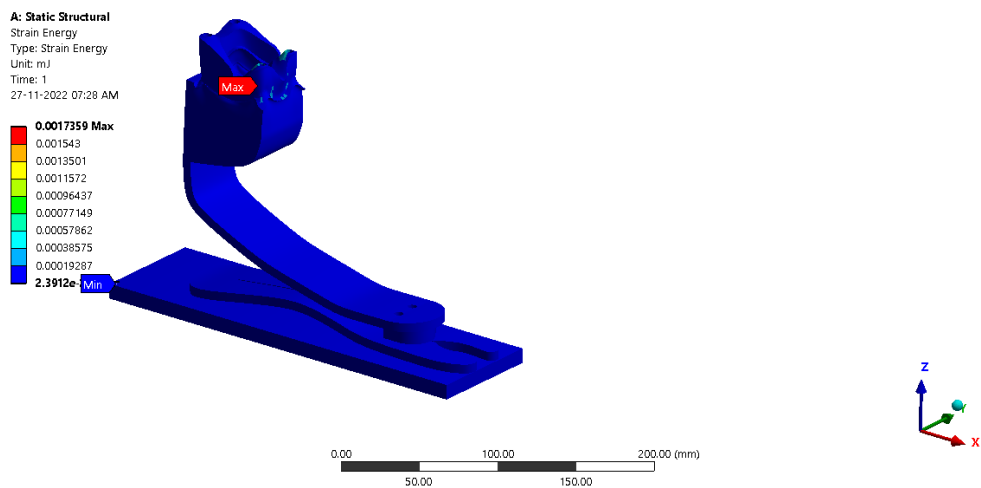


Figure 5.65: Strain energy for prosthetic foot model 4 during mid stance simulation

For prosthetic foot model 5, the mid stance phase was represented by entirely limiting the bottom contact surface to the platen. A same magnitude vertical load was applied to the foot in a downward motion.

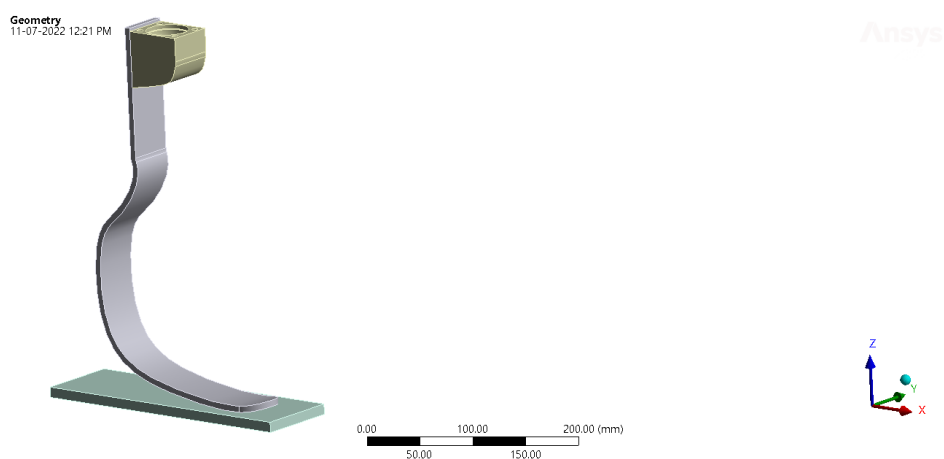


Figure 5.66: Prosthetic foot model 5 geometry during mid stance situation

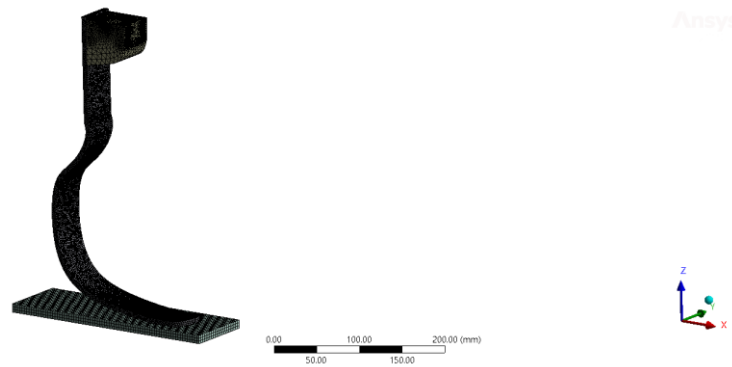


Figure 5.67: Prosthetic foot mesh model 5 during mid stance situation

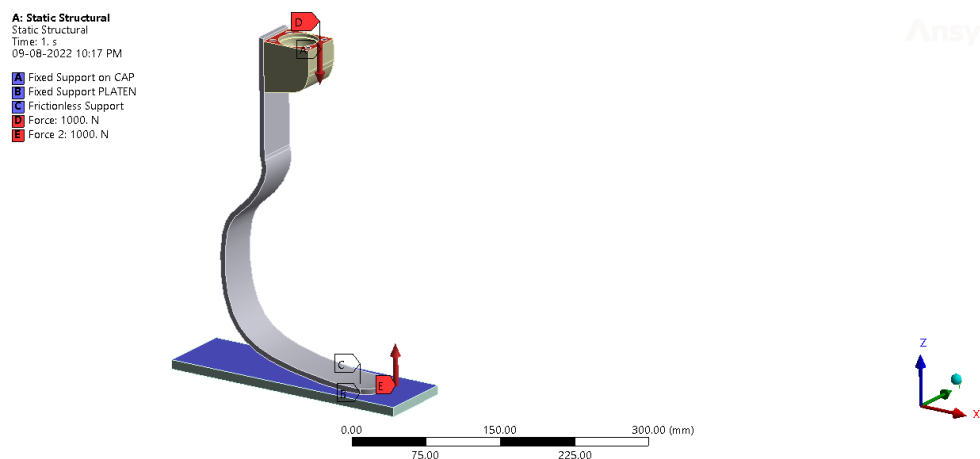


Figure 5.68: Static structural simulation of prosthetic foot model 5 during mid stance situation

Table 5.11: Mid stance analysis on prosthetic foot model 5

Sr no.	Materials	Prosthetic foot model 5			
		Total deformation (Hz)	Total deformation (mm)	Equivalent stress (MPa)	Strain energy (mJ)
1	ABS	115.35	0.011	4.0724	0.001078
2	ABS+PC PLASTIC	114.33	0.01109	4.0724	0.001077
3	ACETAL RESIN	108.76	0.011099	4.0721	0.001076
4	CFRC	168	0.0111	4.0705	0.001065
5	NYLON 6/6	87.363	0.01109	4.0732	0.00108
6	PEEK	129.57	0.011102	4.0716	0.001074
7	PET	111.43	0.01109	4.0721	0.001076
8	PLA	125.53	0.0111	4.0718	0.001075
9	UHMW-PE	351.9	0.011119	4.075	0.0010661

Simulation results data by considering the optimization in the material for the prosthetic foot model 5 was mentioned in Table 5.11. As per the simulated data UHMW-PE material was suitable for the preparation of the prosthetic foot model 5 as per the applied loading situation in the midstance simulation.

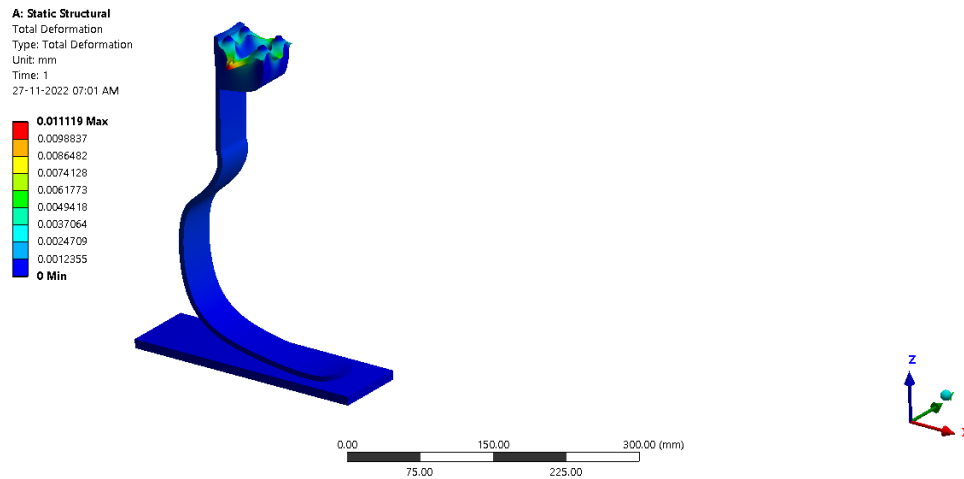


Figure 5.69: Total deformation in mm for prosthetic foot model 5 during mid stance simulation

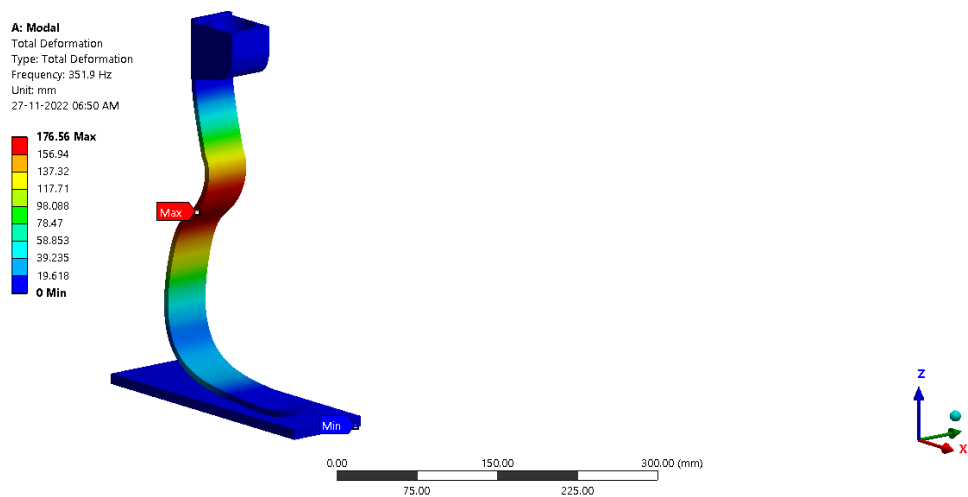


Figure 5.70: Total deformation in Hz for prosthetic foot model 5 during mid stance simulation

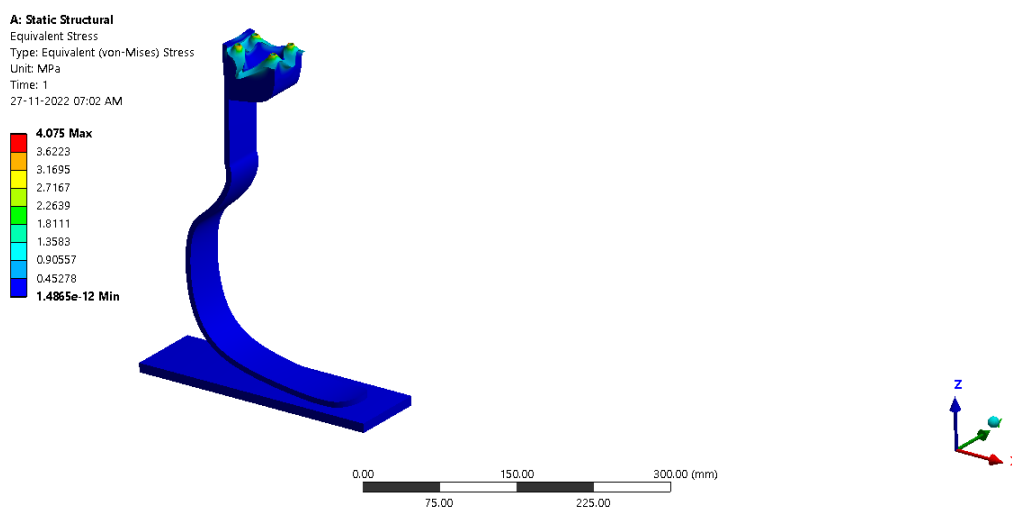


Figure 5.71: Equivalent stress for prosthetic foot model 5 during mid stance simulation

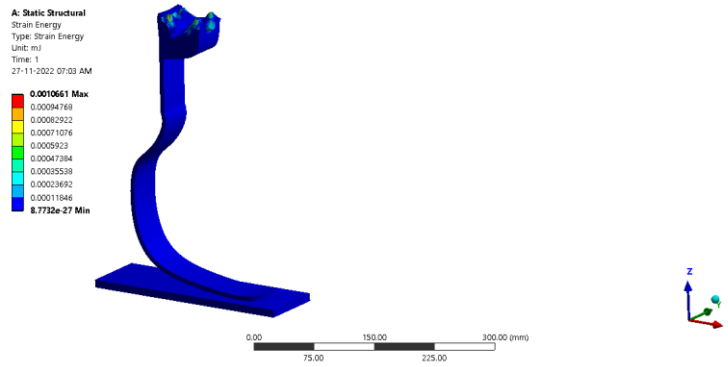


Figure 5.72: Strain energy for prosthetic foot model 5 during mid stance simulation

The mid stance phase was replicated for prosthetic foot model 6 by totally restricting the bottom contact surface to the platen. A same magnitude vertical load was applied to the foot in a downward motion.



Figure 5.73: Prosthetic foot model 6 geometry during mid stance situation

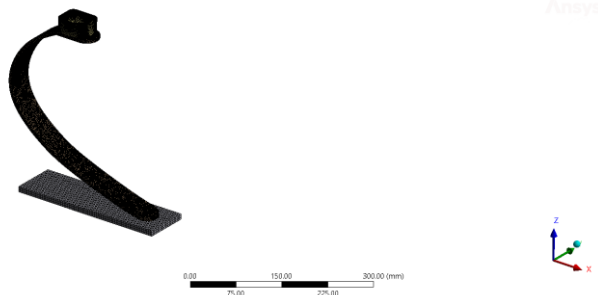


Figure 5.74: Prosthetic foot mesh model 6 during mid stance situation

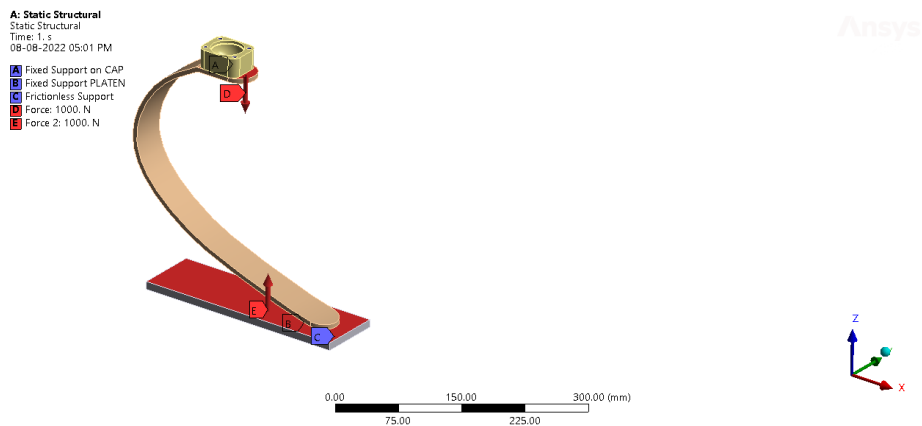


Figure 5.75: Static structural simulation of prosthetic foot model 6 during mid stance situation

Table 5.12: Mid stance analysis on prosthetic foot model 6

Sr no.	Materials	Prosthetic foot model 6			
		Total deformation (Hz)	Total deformation (mm)	Equivalent stress (MPa)	Strain energy (mJ)
1	ABS	71.674	0.061478	7.9646	0.007344
2	ABS+PC PLASTIC	71.076	0.05909	7.8205	0.007229
3	ACETAL RESIN	67.725	0.05297	7.4223	0.006896
4	CFRC	165.25	0.006786	18.127	0.002922
5	NYLON 6/6	54.022	0.091491	9.5511	0.011318
6	PEEK	80.869	0.04215	6.5367	0.0062
7	PET	69.432	0.052739	7.4208	0.006861
8	PLA	78.347	0.045984	6.8977	0.00645
9	UHMW-PE	208.71	0.010744	16.968	0.002732

Simulation results data by considering the optimization in the material for the prosthetic foot model 6 was mentioned in Table 5.12. As per the simulated data, UHMW-PE material was suitable for the preparation of the prosthetic foot model 6 as per the applied loading situation in the midstance simulation.

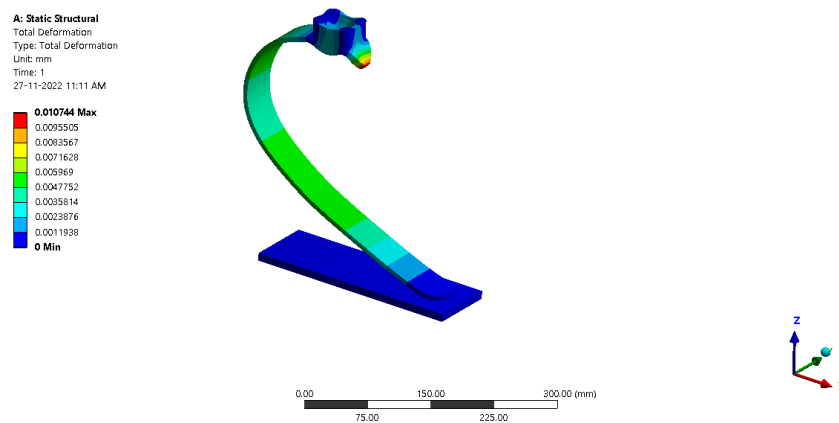


Figure 5.76: Total deformation in mm for prosthetic foot model 6 during mid stance simulation

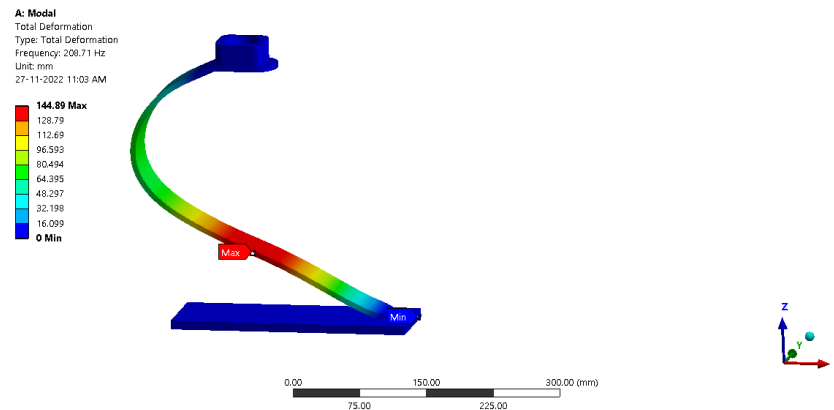


Figure 5.77: Total deformation in Hz for prosthetic foot model 6 during mid stance simulation

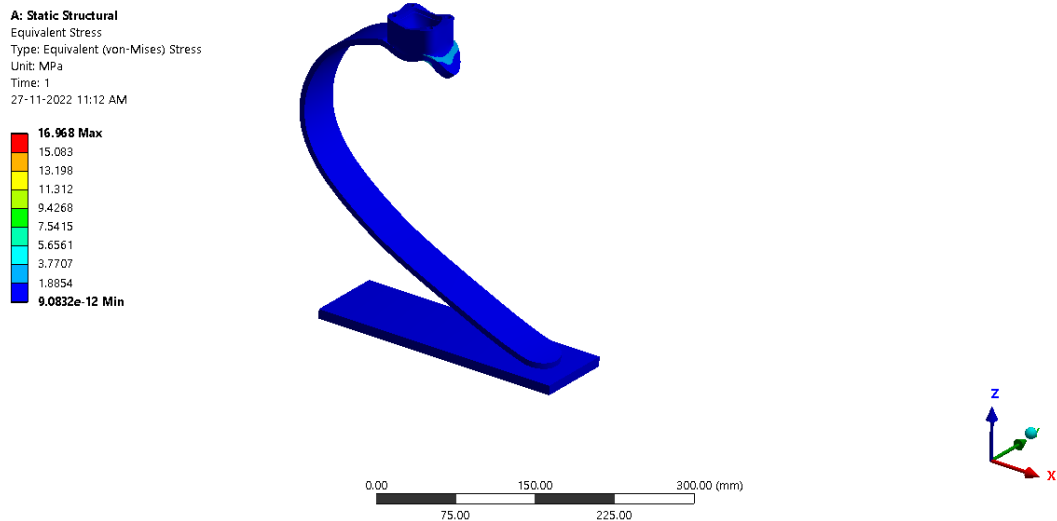


Figure 5.78: Equivalent stress for prosthetic foot model 6 during mid stance simulation

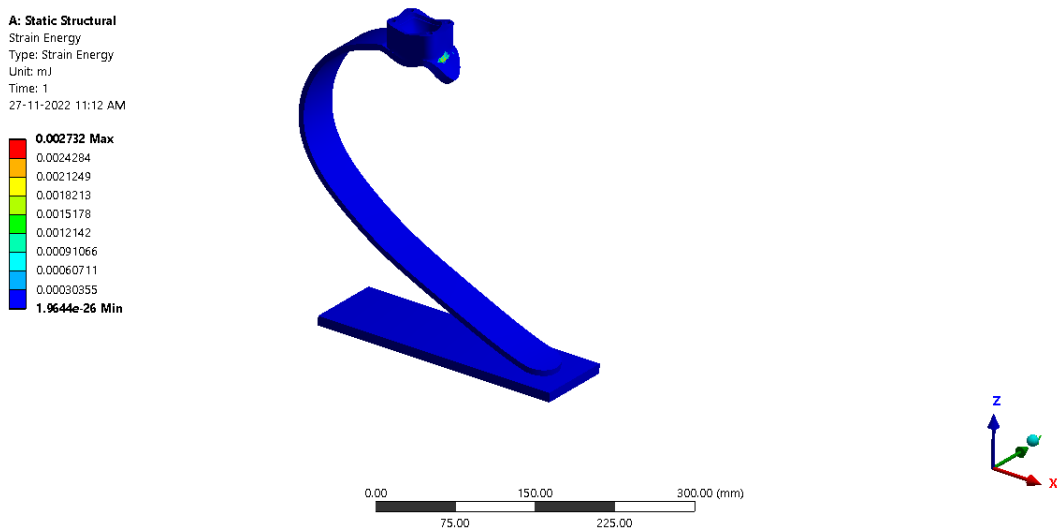
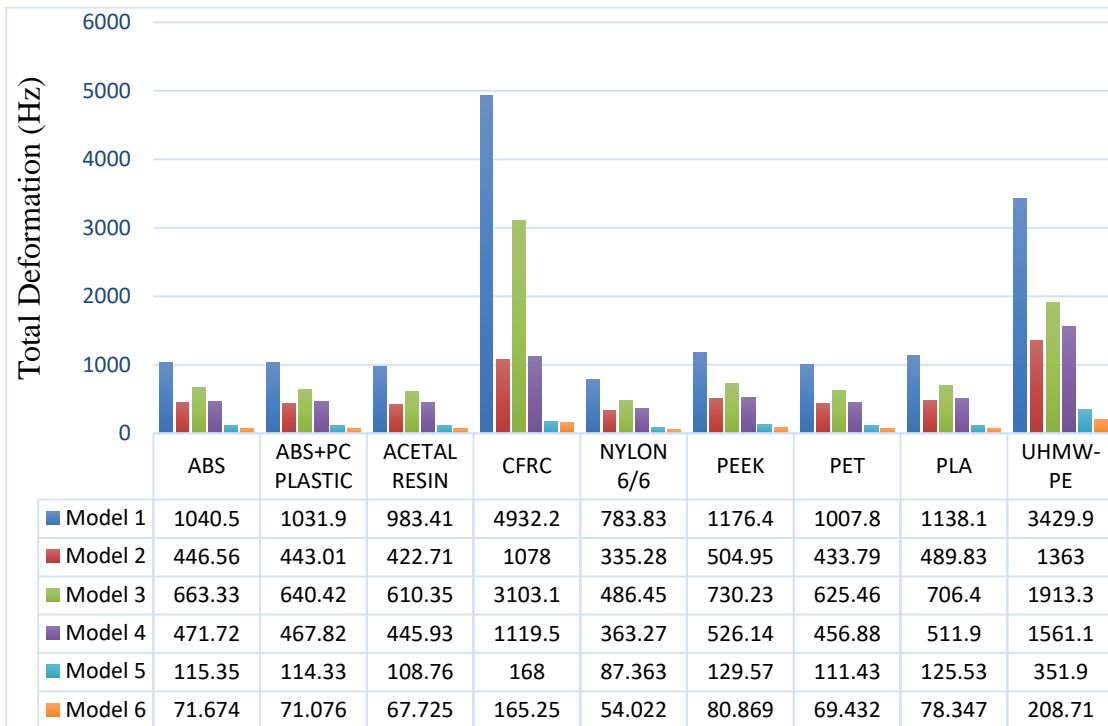


Figure 5.79: Strain energy for prosthetic foot model 6 during mid stance simulation

## 5.5 SIMULATION DATA SUMMARY FOR VARIOUS PROSTHETIC FOOT MODELS

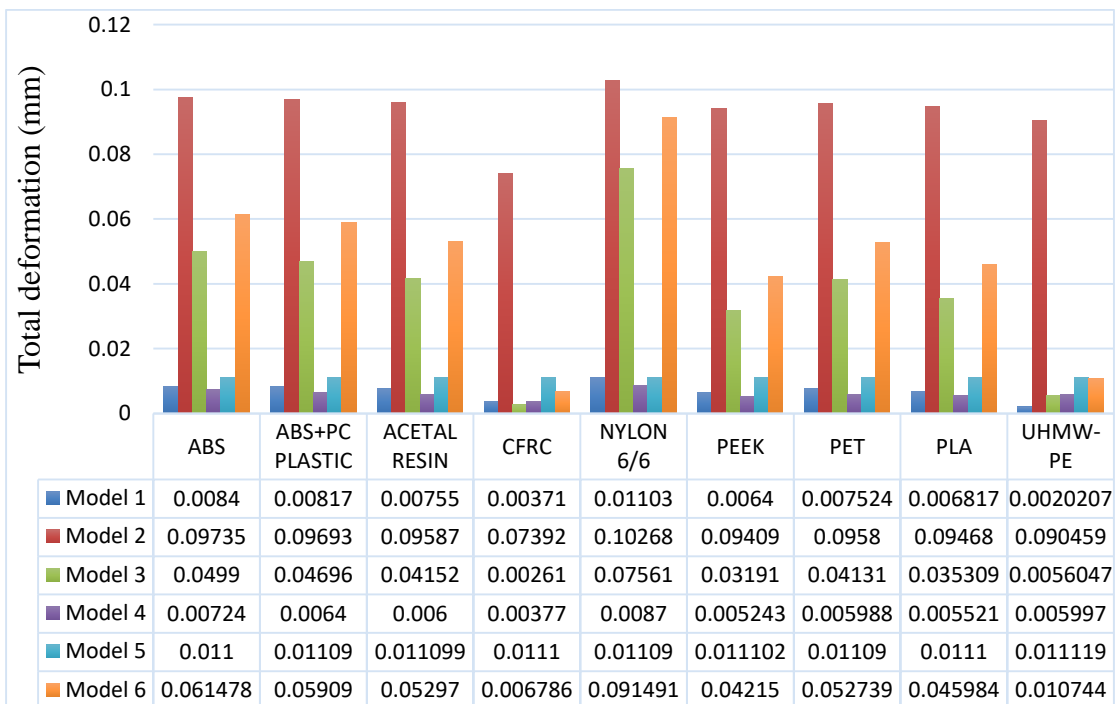
Various parameters analysis was conducted on the foot structure model for material optimization data as shown in tables. An element's frequency response is exclusively connected to its attributes, such as its materials and density (Zhang, et al., 2019). Through modal analysis, the result shows that the natural frequency (1363 Hz) of model 2 was the maximum for UHMW-PE material as shown in Table 5.13. This material can be selected for the preparation of the prosthetic foot model to ensure the best performance.

Table 5.13: Frequency analysis of various foot structure models



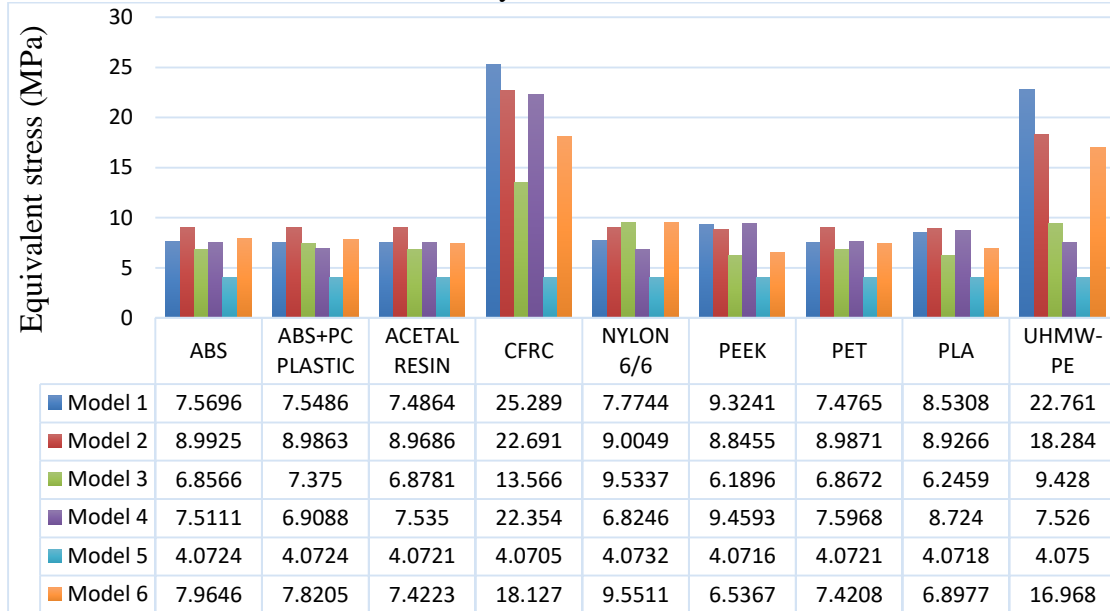
The total deformations by considering different materials of the models were calculated in ANSYS software tools for various configuration models. The minimum total deformation was observed to be 0.002020 mm for UHMW-PE material for prosthetic foot model 1 as mentioned in Table 5.14.

Table 5.14: Deflection analysis of various foot structure models



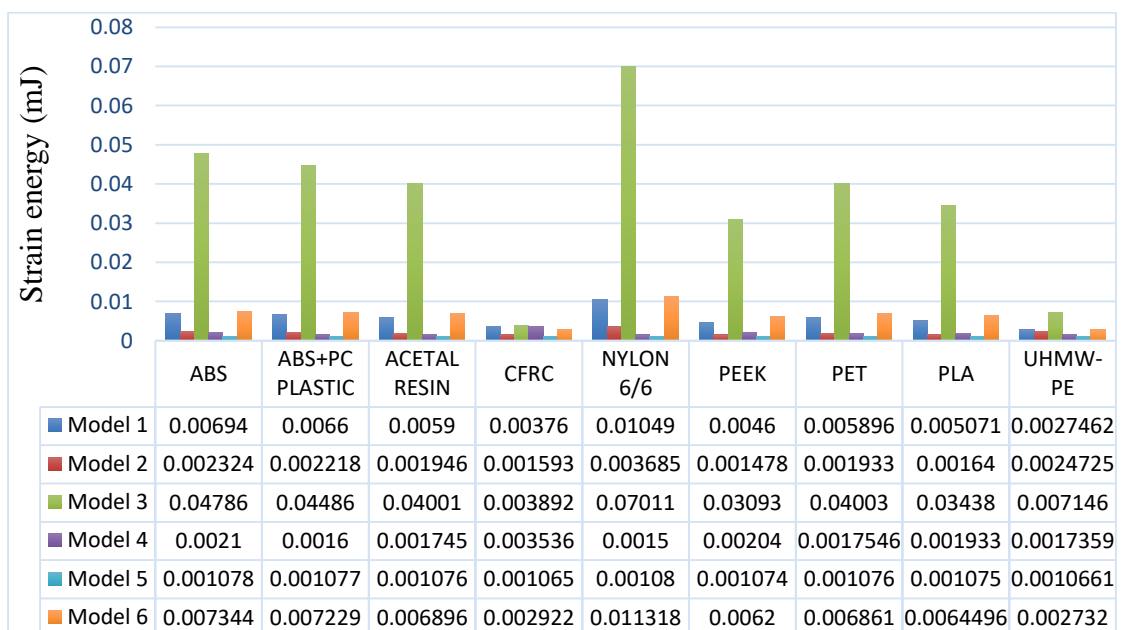
Similarly, von-mises stress was calculated by applying 1000 N for the midstance position of the prosthetic foot structure. The minimum stress was found to be 7.4765 MPa for PET material for prosthetic foot model 1 as mentioned in Table 5.15.

Table 5.15: Stress analysis of various foot structure models



The FEM is a versatile numerical method which allows strain analyses of complex foot structures. Prosthetic feet that conserve energy through midstance movement and restore it throughout late-stance movement are known as energy-storing prosthetic feet. As per the analysis data, the maximum strain energy was found to be 0.01049 mJ for nylon 6/6 material in model 1 as mentioned in Table 5.16.

Table 5.16: Strain energy analysis of various foot structure models



The desirable values of the effective parameters for various prosthetic foot structure models are mentioned in Table 5.17.

Table 5.17: Prosthetic foot model analysis data (mid stance situation)

Sr no.	Effective Parameters	Desirable value	Prosthetic foot model 1	Prosthetic foot model 2	Prosthetic foot model 3	Prosthetic foot model 4	Prosthetic foot model 5	Prosthetic foot model 6
			Material (Value)					
1	Total deformation (Hz)	Maximum	CFRC (4932.2 Hz)	UHMW-PE (1363 Hz)	CFRC (3103.1 Hz)	UHMW-PE (1561.1 Hz)	UHMW-PE (351.9 Hz)	UHMW-PE (208.71 Hz)
2	Total deformation (mm)	Minimum	UHMW-PE (0.002020 mm)	CFRC (0.07392 mm)	CFRC (0.00261 mm)	CFRC (0.00377 mm)	ABS (0.011 mm)	CFRC (0.00678 mm)
3	Strain energy (mJ)	Maximum	Nylon 6/6 (0.01049 mJ)	Nylon 6/6 (0.0036 mJ)	Nylon 6/6 (0.07011 mJ)	CFRC (0.003536 mJ)	Nylon 6/6 (0.00108 mJ)	Nylon 6/6 (0.011318 mJ)
4	Equivalent stress (MPa)	Minimum	PET (7.4765 MPa)	PEEK (8.8455 MPa)	PEEK (6.1896 MPa)	Nylon 6/6 (6.8246 MPa)	CFRC (4.0705 MPa)	PEEK (6.5367 MPa)

This approach may be used in the prosthetic feet design phase to examine the behavior of a prosthetic foot across different walking circumstances.

## 5.6 DESIGN FOR MANUFACTURING OF THE PROSTHETIC FOOT MODEL

The various configuration models of the prosthetic foot were designed and finally, as per the simulation data split type prosthetic foot model 2 was finalized for the manufacturing process.

The present approach relates to foot prosthetics having a lightweight multiaxial foot ankle mechanism design for below-knee amputees in all terrain conditions. The current single-unit prosthetic foot structure can be made from carbon fiber or polymer molded material for cost-effectiveness.

The present approach is based on the principles of Design for Assembly (DFA) and Design for Manufacturing (DFM), (Madu, 2022) where the foot structure is built as a single unit instead of multiple components and complicated structures used previously. The foot structure is flexible to be used for indoor and outdoor activities. The product is easy to handle in terms of usage and also removes the earlier limitations faced by the patient.

Figure 5.80 shows an exploded view of the parts of the multiaxial foot-ankle mechanism to understand the associated connection of the device. The main part of the multiaxial foot-ankle mechanism is the human foot structure which is the base for the stability of the patients and better control in all terrain.

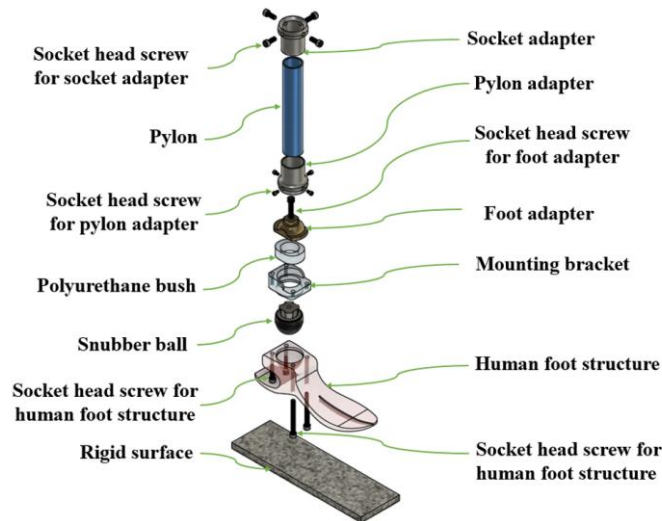
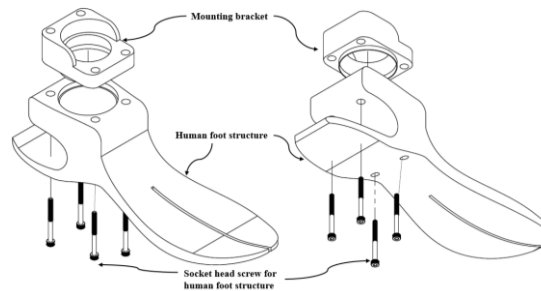


Figure 5.80: Exploded view of the multiaxial foot ankle mechanism

The present approach relates to a prosthetic foot comprising a hollow rectangular lightweight top section that is an integral part of the novel single-unit prosthetic foot structure. The human foot structure assembly comprises two novel components concerning the present disclosure: human foot structure and mounting bracket.

Figure 5.81 visualizes the North-East (NE) and South-East (SE) isometric exploded view of the human foot structure assembly. The major two components; the human foot structure and mounting bracket of the multiaxial foot-ankle mechanism are shown in the North-East and South-West isometric view.



(a) NE isometric view

(b) SE isometric view

Figure 5.81: Exploded view of human foot structure assembly

Figure 5.82 visualizes the transparent view & Figure 5.83 illustrates the perspective view of the human foot structure. The mounting bracket is fixed with the stiff surface portion of the human foot structure through socket head screws for human foot structure that are inserted through holes of large depth and small depths. Similar provisions of holes of large depth and small depth are made on the mounting bracket to connect with the foot structure through socket head screws for the human foot structure. A stiff

surface for the mounting bracket is provided on the top profile of the human foot structure for the functional mobility of lower limb prosthetic users.

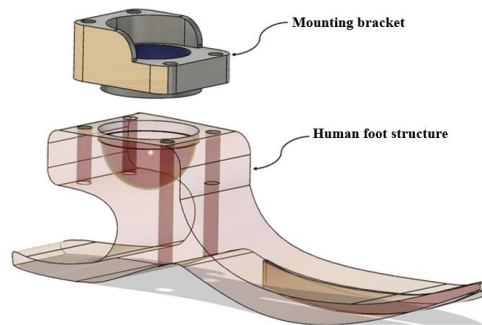


Figure 5.82: Transparent view of human foot structure with mounting bracket

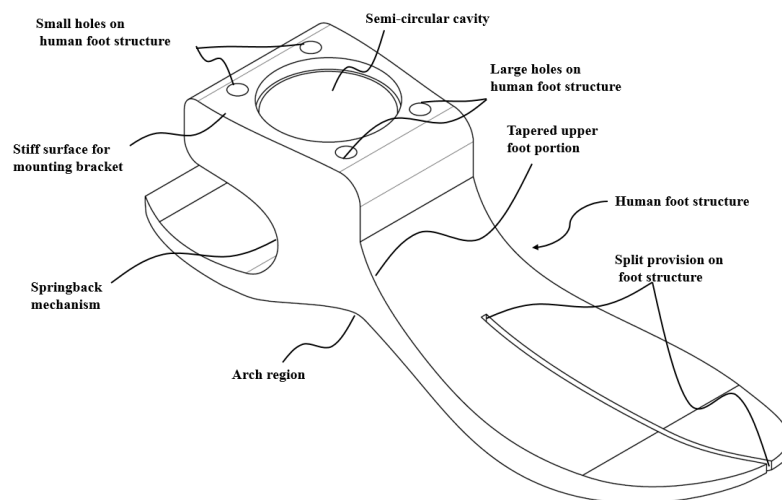


Figure 5.83: Perspective view of human foot structure

Figure 5.84 illustrates the orthographic view wherein four views front, top, side, and bottom of the human foot structure are presented using the first angle projection method.

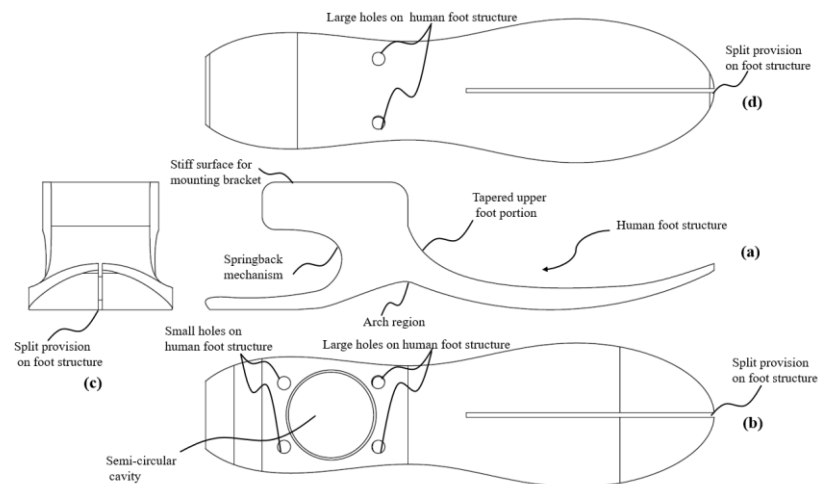


Figure 5.84: Orthographic views of human foot structure assembly (a) Front view (b) Top view (c) Side view and (d) Bottom view

Figure 5.85 represents the NE and SE isometric view of the mounting bracket. The snubber ball is inserted in the region of the snubber ball mounting area within the semi-circular cavity and the mounting bracket for the multiaxial rotation ankle.

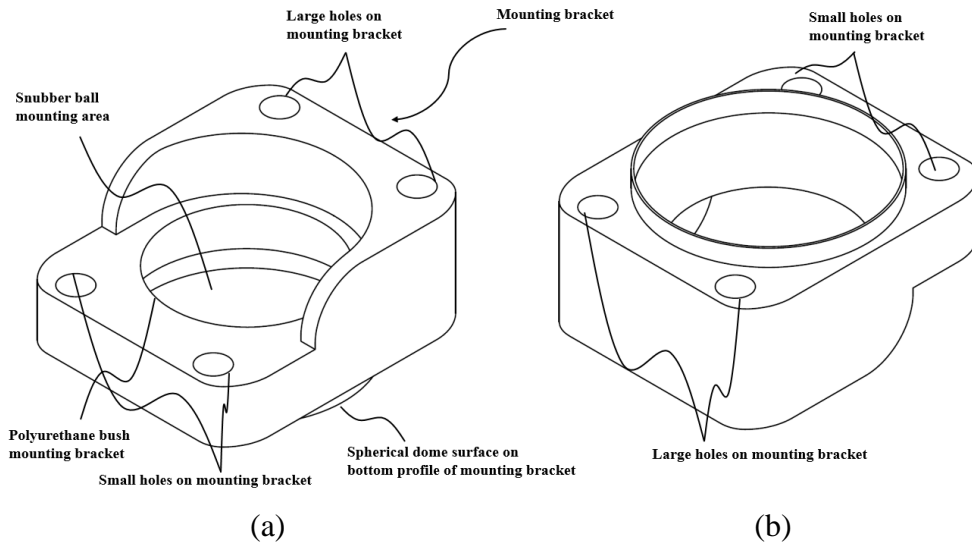


Figure 5.85: NE and SE isometric view of the mounting bracket

Figure 5.86 illustrates the side view of the mounting bracket in the horizontal and vertical directions.

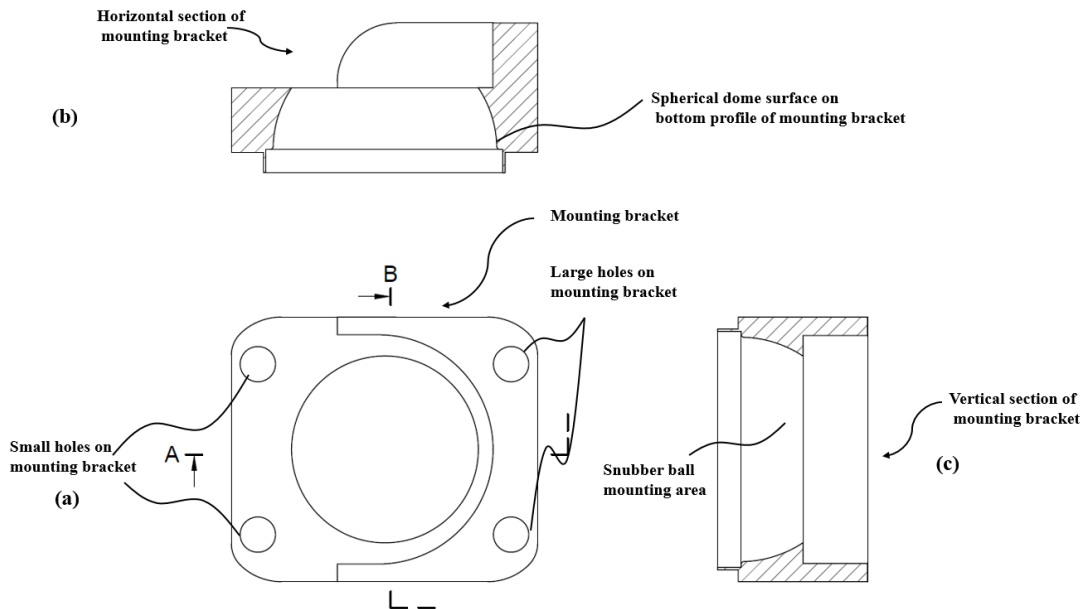


Figure 5.86: Cross-section views top, section A-A and section B-B of the mounting bracket

Elements other than the present development like socket head screw for human foot structure, pylon, foot adapter, polyurethane bush, snubber ball, pylon adapter, socket adapter, socket head screw for foot adapter, socket head screw for pylon adapter, socket

head screw for socket adapter are assembled to get the required functionality. The bottom rigid surface is just for alignment whereas the pylon should always be vertical to  $90^\circ$  for proper weight-bearing distribution.

Figure 5.87 shows the assembled view of the multiaxial foot-ankle mechanism where all the required parts are connected in a sequence to the main human foot structure.

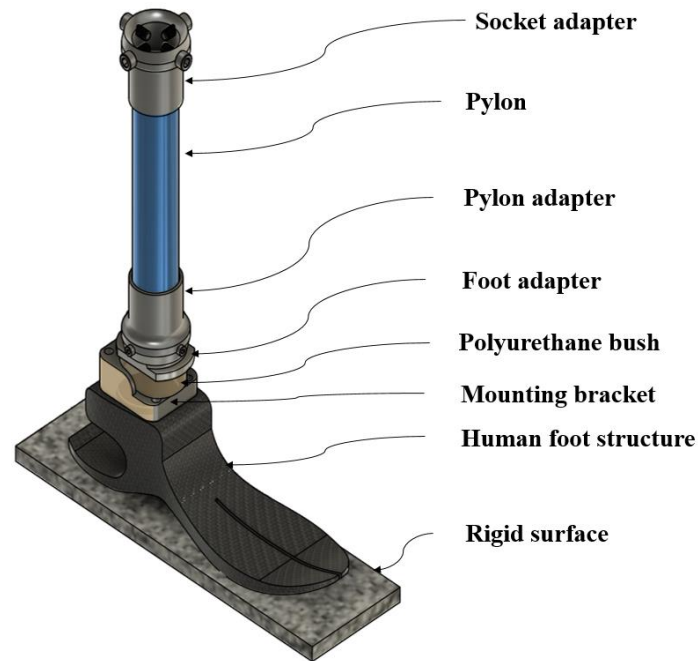


Figure 5.87: Assembly view of the multiaxial foot-ankle mechanism

Figure 5.88 shows the transparent assembled view of the multiaxial foot-ankle mechanism. The snubber ball is inserted in the semi-circular cavity for the multiaxial rotation ankle. The mounting bracket is placed over the snubber ball and is connected to the stiff surface of the mounting bracket by the socket head screw for the human foot structure from the bottom side of the small holes on the human foot structure to the large holes of the mounting bracket and large holes on human foot structure to the small holes on the mounting bracket. The polyurethane bush is inserted into the extended part of the snubber ball up to the polyurethane bush mounting area placed above the mounting bracket to bear the weight. The foot adapter is connected to the snubber ball and fixed with the help of a socket head screw for foot adapter. The pylon adapter is mounted on the foot adapter and tightened with the socket head screw for the pylon adapter at four points. The socket adapter is mounted on the pylon and tightened with the socket head screw for the socket adapter at four points. The pylon joins the socket adapter, with the pylon adapter acting as the human femur and/or tibia and fibula, depending on the amount of amputation.

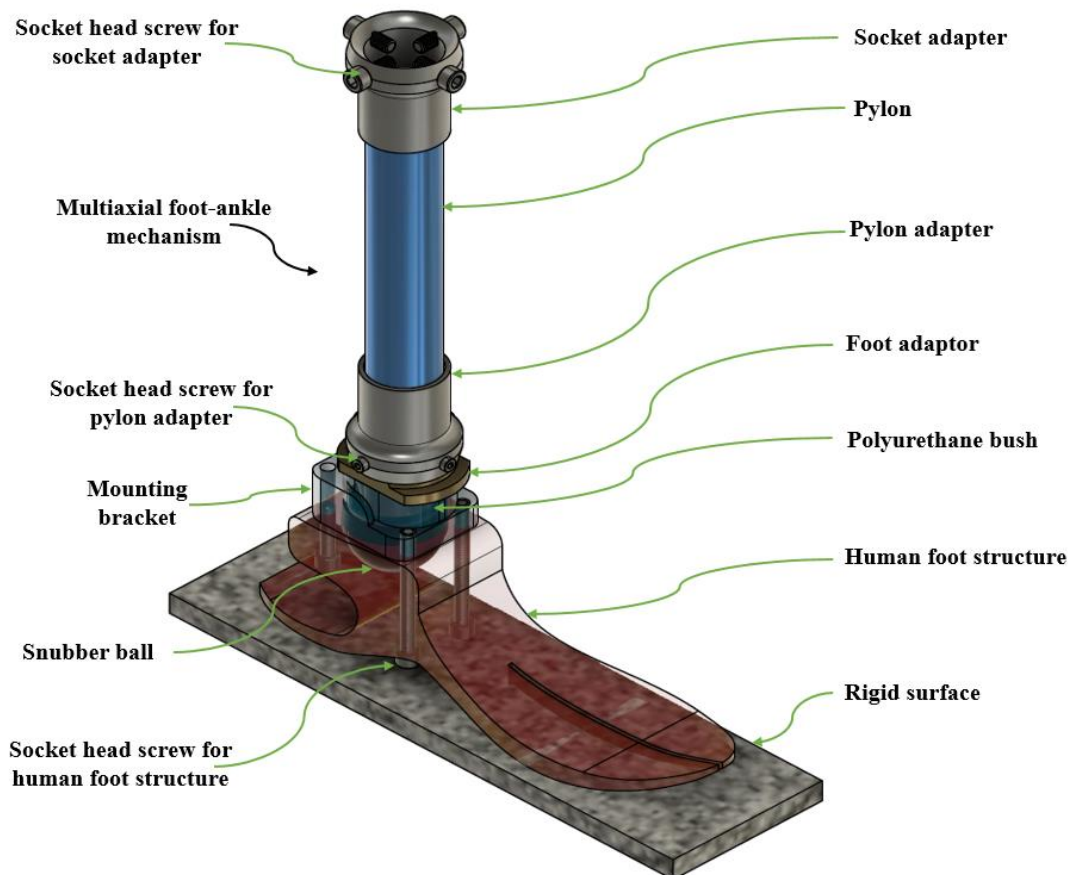


Figure 5.88: Transparent assembly view of the multiaxial foot-ankle mechanism

The polyurethane bush is inserted into the extended part of the snubber ball up to the polyurethane bush mounting area placed above the mounting bracket to bear the weight. The foot adapter is connected to the snubber ball and fixed with the help of a socket head screw for foot adapter. The pylon adapter is mounted on the foot adapter and tightened with the socket head screw for the pylon adapter at four points.

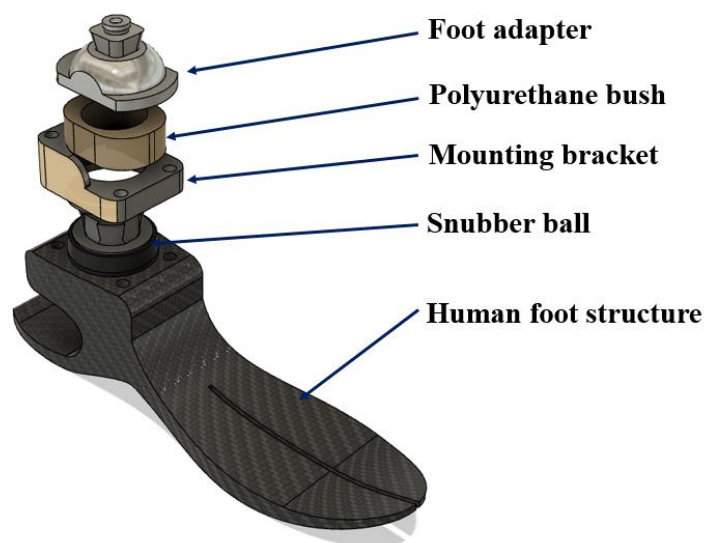


Figure 5.89: Human foot structure assembly

Figure 5.90 depicts a transparent view of a human foot structure constructed according to the principles of the current approach, in which the human foot structure, mounting bracket, socket head screw for the human foot structure, polyurethane bush, and snubber ball are all assembled.

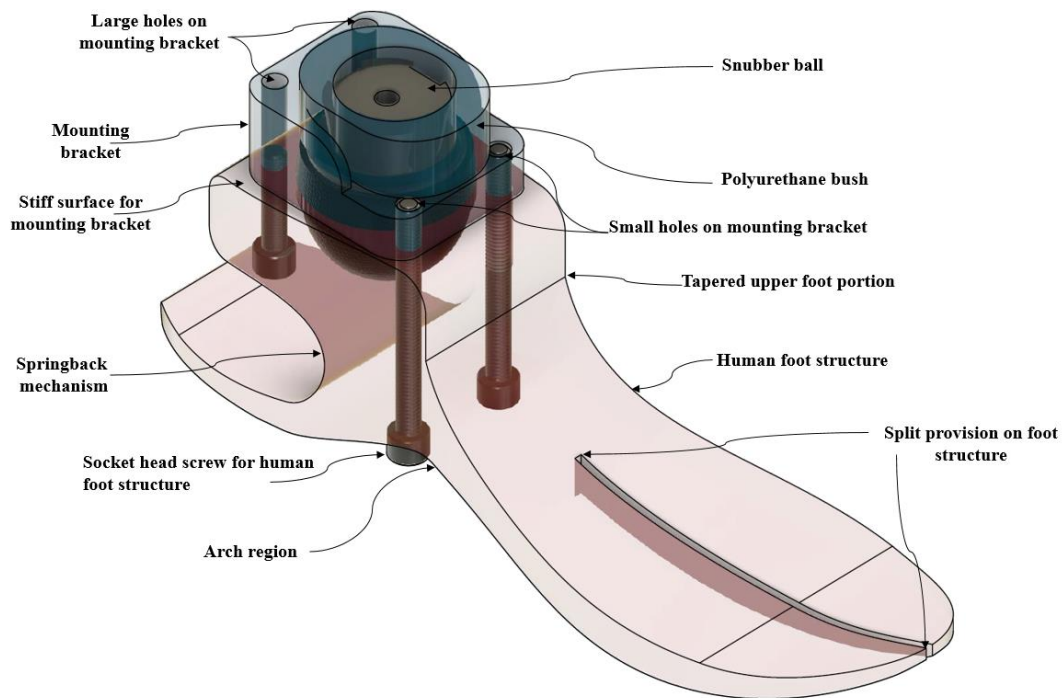


Figure 5.90: Perspective transparent view of human foot structure assembly

The present design approach is associated with a multi-axial foot-ankle mechanism for prosthetic legs that allows the user to walk on steps or uneven terrain without losing balance while maintaining the stability of the structure. The present approach is made of lightweight material having a foot portion and an attached ankle portion capable of a desired degree of rotation concerning the prosthetic frame. The approach is an optimization in the prosthetic foot structure design that resembles the human foot surface.